C.P. No. 147
(15,429)
A.R.C. Technical Report

MINISTRY OF SUPPLY

AERONAUTICAL RESEARCH COUNCIL
CURRENT PAPERS

Theoretical Load Distributions on Wings with Cylindrical Bodies at the Tips

By

D. E. Hartley

LONDON: HER MAJESTY'S STATIONERY OFFICE

1954

Price 3s. 6d. net

C.P. No.147

Addendum to
Report No. Aero 2469

June, 1952.

ROYAL AIRCRAFT ESTABLISHMENT

Theoretical Load Distributions on Wings
with Cylindrical Bodies at the Tips

by

D.E. Hartley, B.A.

ADDENDUM

From theoretical reasoning, in connection with the load on a wing with one cylindrical body at one end (Reference 7), it has been suggested to replace equation (49) for the effective aspect ratio of the wing-body combination by the following relation:-

$$\frac{A_e}{A} = 1 + \frac{D}{b}$$

With this relation, the theoretical estimates obtained from the present method agree well with experimental results, as shown in an unpublished report by Spence and Holford.

C.P. No.147

Report No. Aero 2469

June, 1952.

ROYAL AIRCRAFT ESTABLISHMENT

Theoretical Load Distributions on Wings with Cylindrical Bodies at the Tips

by

D.E. Hartley, B.A.

SUMMARY

The effect of tip-tanks on spanwise lift distributions is investigated theoretically for the case of minimum induced drag in incompressible potential flow.

Charts enabling rapid estimation of the changes in span loadings, total lifts and induced drags are presented for a practical range of the ratio of tank diameter to wing span.

It is shown how the results may be applied approximately to wings of any planform, including those with sweep or of low aspect ratio.

LIST OF CONTENTS

LIST OF ILLUSTRATIONS

LIST OF SYMBOLS

x, y, z	rectangular co-ordinates of the physical space; x in free stream direction, y sideways, z downwards
$\zeta = z + iy$	co-ordinate in the physical z-y plane
$\zeta_\nu = z_\nu + iy_\nu$	co-ordinate in the transformed planes
where $\nu = 1, 2, 3, 4, 5$ or 6	
D	tank diameter
b	wing span, excluding the tanks
c	local chord
$\bar{c}$	mean chord
A	aspect ratio
A_e	effective aspect ratio
φ	mean sweepback angle of the half-chord line
φ_e	effective sweepback angle
t/c	wing thickness-chord ratio
α	geometric wing incidence
α_i	induced incidence due to the trailing vortex system
$\Delta\alpha_T$	upwash incidence due to flow across the isolated tanks
R	Reynolds number
V_0	free stream velocity
v	velocity
$v_{z\infty}$	downwash velocity far downstream due to the trailing vortices
$\omega = \dfrac{2\alpha_i V_0}{v_{z\infty}}$	downwash factor
W	potential function defined in Appendix (Eq. A2)
$\Phi = \phi + i\psi$	complex potential function
Γ	circulation
C_L	local lift coefficient
$\bar{C}_L$	mean total lift coefficient
$\bar{C}_{L_W}$	mean wing lift coefficient
$\bar{C}_{L_E}$	mean lift coefficient on an elliptical wing alone

LIST OF SYMBOLS (contd)

a	section lift-curve slope
$n = \frac{\omega}{2}$	coefficient occurring in the calculation of 'ω' and 'a'
J, J_W, J_T	functions related to the total lift, wing lift and tank lift respectively

Suffices

US	upper surface
LS	lower surface
w	wing (tanks present)
T	tanks
E	elliptical wing alone
e	effective
J	junction
∞	infinity

1 Introduction

At the present time a considerable amount of attention is being given to the problems associated with the carriage of external stores such as fuel tanks and, amongst other aerodynamic effects, it has been observed that tip-tanks give rise to large increments in lift. The present paper provides a method of estimating the magnitude and spanwise distribution of such increments.

The calculations relate to wings without camber or twist and fitted with two equal, circular-cylindrical tip-tanks situated symmetrically with respect to the plane of the wing.

Incompressible potential flow is assumed and only the case of minimum induced drag (with the tip-tanks in position) is considered - that is, the calculations strictly refer to one particular set of planforms.

The problem is attacked by the method developed by M.M. Munk[1], L. Prandtl[2] and E. Trefftz[3] and adopted by W. Mangler[4,5] in his work on aerofoils with endplates.

It is assumed that the velocity $\alpha_1 V_0$ induced at the aerofoil by the trailing vortices is constant, and that the vortex sheet far behind the aerofoil moves downwards with a constant velocity $v_{z\infty}$. The lift forces are deduced in section 4 from the velocity potential on the vortex sheet far downstream in terms of $v_{z\infty}$ and the relationships between circulation, induced incidence and lift-curve slope existing on the aerofoil serve to determine $v_{z\infty}$. Calculation of the potential function far downstream is essentially the problem of finding the two-dimensional flow past a solid boundary shaped like a cross-section of the vortex sheet. Conformal transformations enabling this to be done in the present case were found (section 2) to be already existing in a report[6] by I.E. Garrick on the potential flow about biplane aerofoils and in W. Mangler's work[4,5] on aerofoils with endplates.

A problem closely related to the present one - the loading on a rear fuselage and fin, which for small values of the ratio of fuselage diameter to fin span may be looked upon as a wing with one tip-tank - has been solved[7] by J. Weber, concurrently with the present work. Here again the minimum induced drag problem has been studied; there is little likelihood that non-minimum solutions will be forthcoming for either problem. H. Multhopp's general solution of the loading on a wing with a fuselage (extended[8] by J. Weber to take sweepback into account) is a particular case in which a transformation could be used leading to boundary conditions exactly the same as those for a wing alone; similar cases will obviously not occur frequently.

The possibilities of applying the present solutions to wings of arbitrary planform, including low aspect ratio and sweep, are discussed in section 6.

A numerical procedure, suitable for practical applications of the results, is outlined in section 7 and Table I.

2 Conformal Transformations

In the physical space, a rectangular co-ordinate system x,y,z is taken; x is measured in the free stream direction, y to starboard and z vertically downwards.

A wing is considered which has a span b , mean chord $\bar{c}$ and aspect ratio A , together with tip-tanks which are basically circular cylinders of diameter D. The wing is assumed thin, with no camber or twist and of a planform such as to give minimum induced drag when in conjunction with the tanks. Fig.1 shows a wing with tip-tanks and a part of the downstream vortex system. Fig.2 shows a cross-section of the vortex sheet far downstream, perpendicular to the stream direction, and it is desired to calculate the potentials on this surface when it moves downwards with velocity $v_{Z\infty}$. As a step towards this goal, the flow must first be obtained for a streaming motion past the stationary object. The state of affairs is shown in Fig.3(i). Since the potential function for this motion is not known, conformal transformations must be made until a shape is obtained for which the potential function of the corresponding flow is available.

The transformations are in two main groups: the first group, which is taken from a report[6] by I.E. Garrick, transforms the shape of Fig.3(i) in that corresponding to a wing with endplates (Fig.3(ii)), and the second group, transformations of W. Mangler[4,5], converts the aerofoil-endplates configuration into a straight line (Fig.3(iii)). A parallel stream at infinity in the physical plane becomes the flow due to a doublet on the axis in the final stage of the transformations.

The complex co-ordinate ζ_ν is used in the transformed planes where

$$\zeta_\nu = z_\nu + iy_\nu$$

$$\text{and} \qquad \nu = 1,2,3,4,5 \text{ or } 6 \,;$$

in the physical plane the corresponding co-ordinate is ζ where

$$\zeta = z + iy \,.$$

In the figures showing the various planes, corresponding points are denoted by the same letter but with appropriate suffices. Geometrical proportions have been maintained roughly between Figs. 4 and 7 and between Figs. 8, 9 and 10.

The transformations will now be described briefly, with some attention being paid to points arising out of their particular application to the present problem where the tank diameter is small compared with the wing span. A list of the symbols is given at the beginning of the Report.

(i) By the transformation

$$\frac{\zeta_1}{s} = \frac{\zeta + is}{\zeta - is} \tag{1}$$

the whole of the ζ-plane (Fig.4) external to the circles K and K' is transformed into the annular region between two concentric circles K_1 and K_1' in the ζ_1-plane (Fig.5).

The derivation of the transformation may be understood if, in the ζ-plane, the circles K and K' are considered members of a coaxial system of circles with limiting points at Q and Q' and if Q and Q' are taken as origins for two polar co-ordinate systems (ρ, δ) and (ρ', δ'). Q and Q' are the points $\pm$ is, where

$$s = \sqrt{\frac{b}{2}\left(\frac{b}{2} + D\right)} \tag{2}$$

and are close to the centres O and O' of K and K'.

Any point in the ζ-plane may then be written

$$\zeta = z + iy = is + \rho\, e^{i\delta} = -is + \rho'\, e^{i\delta'}$$

and so from equation (1)

$$\frac{\zeta_1}{s} = \frac{\zeta + is}{\zeta - is} = \frac{\rho'}{\rho}\, e^{i(\delta'-\delta)}$$

Using polar co-ordinates (r_1, θ_1) with the origin at $y_1 = 0$

$$y_1 = r_1\, e^{i\theta_1}$$

and
$$r_1 = s\,\frac{\rho'}{\rho}\,, \qquad \theta_1 = \delta' - \delta\,. \tag{3}$$

Thus the coaxial circles ρ'/ρ = constant become the concentric circles r_1 = constant in the ζ_1-plane and the orthogonal system of circles (such as P P' P" P"') are transformed into the straight lines θ_1 = constant (e.g. $P_1\, P_1'''\, P_1''\, P_1'$).

In particular for the circles K and K'

$$r_1 = s\, e^{\pm\beta}$$

where
$$\beta = \cosh^{-1}\left(1 + \frac{b}{D}\right) \tag{4}$$

and the points C and E, vertically above and below O, transform into C_1 and E_1 on K_1 at

$$\theta_1 = \mp \tan^{-1}\left(\frac{2s}{D}\right).$$

(ii) By the transformation

$$\underline{\zeta_2 = i \log\left(\frac{\zeta_1}{s}\right)} \tag{5}$$

the whole of the ζ_1-plane is mapped onto an infinite number of strips of width 2π and parallel to the imaginary axis in the ζ_2-plane (Fig.6). The region external to the circles K_1 and K_2 in the ζ-plane becomes a rectangular region on each of these strips. Attention will be confined to the strip of the ζ_2-plane between the lines $z_2 = \pm\pi$.

Since

$$\zeta_2 = i \log\left(\frac{\zeta_1}{s}\right) = i \log\left[\frac{r_1}{s}\, e^{i\theta_1}\right] = i \log \frac{r_1}{s} - \theta_1$$

$$z_2 = -\theta_1\,; \qquad y_2 = \log\left(\frac{r_1}{s}\right). \tag{6}$$

Thus the concentric circles r_1 = constant in the ζ_1-plane become straight lines parallel to the real axis in the ζ_2-plane and the straight lines θ_1 = constant remain straight lines parallel to the imaginary axis.

The point at infinity in the $\bar{\zeta}$-plane, which corresponds to H_1 ($\zeta_1 = s$) in the ζ_1-plane, is transformed into the origin H_2 in the ζ_2-plane.

(iii) By the transformation *

$$\underline{\zeta_3 = -2\,[Z(\zeta_2) + Z(\zeta_2 + 2i\beta)] - i} \tag{7}$$

the rectangular region in the ζ_2-plane which corresponds to the region external to K and K' in the ζ-plane is transformed into the whole of the ζ_3-plane external to the figure $A_3B_3C_3D_3E_3F_3G_3$ and its reflection in the z_3-axis (Fig.7). This is the end of the first stage of the transformations corresponding to Fig.3(ii): the shape of a section through the trailing vortex system of a wing with tip-tanks has been transformed into the corresponding shape for an aerofoil with endplates.

The relationships between points in the ζ_2 and ζ_3-planes are as follows:

$$\zeta_3 = -2\,[Z(\zeta_2) + Z(\zeta_2 + 2i\beta)] - i$$

where $$Z(\zeta_2) = \tfrac{1}{2}\cot\left(\frac{\zeta_2}{2}\right) + 2\sum_{\ell=1}^{\ell=\infty}\sum_{m=1}^{m=\infty} e^{-4\beta\ell m}\sin(m\,\zeta_2)\,. \tag{8}$$

Splitting this into real and imaginary parts,

$$\left.\begin{aligned} z_3 &= -2\,[M(z_2, y_2) + M(z_2, y_2 - 2\beta)] \\ y_3 &= -2\,[N(z_2, y_2) + N(z_2, y_2 - 2\beta)] \end{aligned}\right\} \tag{9}$$

where **

$$M(z_2,y_2) = \frac{\sin z_2}{2(\cosh y_2 - \cos z_2)} + 2\sum_{\ell=1}^{\ell=\infty}\sum_{m=1}^{m=\infty} e^{-4\beta\ell m}\sin(mz_2)\cosh(my_2)$$

$$N(z_2,y_2) = -\frac{\sinh z_2}{2(\cosh y_2 - \cos z_2)} + 2\sum_{\ell=1}^{\ell=\infty}\sum_{m=1}^{m=\infty} e^{-4\beta\ell m}\cos(mz_2)\sinh(my_2)$$

---

* Z is an elliptic function of the first kind, the zeta-function of Jacobi and Hermite, and its expansion is given later in section (iii).

** It would appear that in Ref.6 algebraic errors have arisen in the expressions for M and N in passing from equation (23) to equation (25). The expressions quoted above differ from those of equation (25) of Ref.6 in having the factor 2 in front of the infinite series terms and in having a positive sign in front of the first term in the expression for $M(z_2,y_2)$.

In particular along $B_3\ C_3\ D_3\ E_3\ F_3$

$$z_3 = -4M(z_2,\beta), \qquad y_3 = 1 \tag{10}$$

and the point H_2, the origin of the ζ_2-plane, becomes the point at infinity in the ζ_3-plane.

As the tank size tends to zero ($^{2D}/b \to 0$, $\beta \to \infty$) the ratio of the infinite series terms to the other terms in the expressions for z_3 and y_3 also tend to zero, the semi-height of the endplate tends to D/s and the extreme points C_3 and E_3 correspond exactly to the points C and E.

For tanks of finite size we may write

$$M(z_2,y_2) = \frac{\sin z_2}{2(\cosh y_2 - \cos z_2)} + 2e^{-4\beta} \sin z_2 \cosh y_2 + O(e^{-8\beta + 2y_2})$$

$$N(z_2,y_2) = -\frac{\sinh z_2}{2(\cosh y_2 - \cos z_2)} + 2e^{-4\beta} \cos z_2 \cosh y_2 + O(e^{-8\beta + 2y_2}) \tag{11}$$

where the third term will always be negligible but where the second term may need to be considered.

For the maximum size of tank taken in the numerical work of this report, the first terms of the series (the second terms in equation (11)) contribute 0.4% and -0.9% to the endplate height and wing semi-span respectively. For tanks equal in diameter to the semi-span, the values would still be only 2.9% and -5.9%. Conditions are not very different therefore from the limiting case $^{2D}/b \to 0$ and in Figs. 4 and 7 the points C and C_3 are shown in positions which strictly only correspond to each other in the limiting case.

(iv)* The transformation

$$\zeta_3 = i\sqrt{\frac{\zeta_4}{i}} \tag{12}$$

transforms one half of the ζ_3-plane (Fig.8) into the whole of the ζ_4-plane (Fig.9) in such a way that the points H_3 at infinity on the z_3-axis become the point H_4 at minus-infinity on the y_4-axis and the endplate is transformed into a parabolic arc.

Since

$$\zeta_3 = i\sqrt{\frac{\zeta_4}{i}}$$

then
$$y_4 = {y_3}^2 - {z_3}^2, \qquad z_4 = 2y_3z_3. \tag{13}$$

Thus the length $A_4\ B_4$ remains equal to the length $A_3\ B_3$ whilst the vertical distance $C_4\ B_4$ is $2K_o$ where K_o is the length $C_3\ B_3$.

*The transformations (iv), (v) and (vi) differ in form from W. Mangler's transformations[4,5] owing to a negative rotation of all axes through $\pi/2$.

Before the next transformation is made, the parabolic arc $C_4 E_4$ is approximated by an arc of a circle passing through C_4, D_4 and E_4 with its centre at $[0, -i(1 + K_o^2/2)]$. The error in this approximation is small for the size of tanks taken in the calculations of this report, but for larger tanks, say $2D/b > 1$,* further consideration must be given to it.

(v) The transformation

$$\zeta_4 = \frac{(3 + K_o^2)\,\zeta_5}{4 + K_o^2 + i\zeta_5} \tag{14}$$

transforms the circle in the ζ_4-plane into a straight line, of which $C_5 D_5 E_5$ is a part, in the ζ_5-plane (Fig.10).

By separating equation (14) into real and imaginary parts,

$$z_4 = \frac{(3+K_o^2)(4+K_o^2)\,z_5}{(4+K_o^2-y_5)^2 + z_5^2}$$

$$y_4 = \frac{(3+K_o^2)\,[y_5(4+K_o^2-y_5) - z_5^2]}{(4+K_o^2-y_5)^2 + z_5^2} \quad . \tag{15}$$

In particular

$$B_5 = 1$$
$$C_5 = i - \frac{K_o}{2}(3+K_o^2)$$

and the point H_4 at $-i\infty$ in the ζ_4-plane becomes the point H_5 at $i(4+K_o^2)$ in the ζ_5-plane.

(vi) By the transformations

$$\frac{\zeta_5}{i} = 1 - \frac{\left(1 + \frac{1}{\zeta_6}\right)}{\left(1 + \frac{1}{g_o}\right)}\sqrt{\frac{\left(g_1 - \frac{\zeta_6}{i}\right)\left(\frac{1}{g_1} - \frac{\zeta_6}{i}\right)}{(g_1 - g_o)\left(\frac{1}{g_1} - g_o\right)}}$$

for $y_6 < g_1$, i.e. along AB

$$\frac{\zeta_5}{i} = 1 + \frac{\left(1 + \frac{i}{\zeta_6}\right)}{\left(1 + \frac{1}{g_o}\right)}\sqrt{\frac{\left(g_1 - \frac{\zeta_6}{i}\right)\left(\frac{1}{g_1} - \frac{\zeta_6}{i}\right)}{(g_1 - g_o)\left(\frac{1}{g_1} - g_o\right)}}$$

for $y_6 > \frac{1}{g_1}$, i.e. along FG

* Such cases may arise in the application of the method to the problem of wings with nacelles (see section 8).

and
$$\frac{\zeta_5}{i} = 1 + i \frac{\left(1 + \frac{i}{\zeta_6}\right)}{\left(1 + \frac{1}{g_o}\right)} \sqrt{\frac{\left(\frac{\zeta_6}{i} - g_1\right)\left(\frac{1}{g_1} - \frac{\zeta_6}{i}\right)}{(g_1 - g_o)\left(\frac{1}{g_1} - g_o\right)}} \qquad (16)$$

for $\frac{1}{g_1} \geq y_6 \geq g_1$, i.e. along BCDEF

the ζ_5-plane is transformed into the upper half of the ζ_6-plane (Fig.11) whilst the figure $A_5B_5C_5D_5E_5F_5G_5$ becomes a part of the y_6-axis.

The relationships (16) are simpler than those given[4,5] by W Mangler owing to the symmetry of our 'endplates' with regard to the imaginary axis and since the endplates are always at the tips of the wings.

The coefficients g_1 and g_2 are related to each other by

$$1 + g_2 + \frac{1}{g_2} = \frac{1}{2}\left(g_1 + \frac{1}{g_1}\right) \qquad (17)$$

and to the endplate height by

$$K_o = \left(1 + \frac{1}{g_2}\right) \sqrt{\frac{(g_2 - g_1)\left(\frac{1}{g_1} - g_2\right)}{(g_1 - 1)\left(\frac{1}{g_1} - 1\right)}} \, . \qquad (18)$$

The constant g_o is then obtainable from

$$3 + K_o^2 = \frac{2}{\left(1 + \frac{1}{g_o}\right)} \sqrt{\frac{(g_1 - 1)\left(\frac{1}{g_1} - 1\right)}{(g_1 - g_o)\left(\frac{1}{g_1} - g_o\right)}} \, . \qquad (19)$$

In any particular calculation, K_o is known from the first three transformations, so equations (17) and (18) must be solved by trial and error for g_1 and g_2 and similarly with equation (19) for g_1.

From the relationships (16) it may be shown that corresponding points on the upper and lower surface of the figure $A_5B_5C_5D_5E_5F_5G_5$ are related in the ζ_6-plane by

$$(y_6)_{US} = \left(\frac{1}{y_6}\right)_{LS} . \qquad (20)$$

The point at infinity in the ζ-plane is transformed into the point H_6 on the imaginary axis at $y_6 = 1$.

The ζ_6-plane is the last stage of the transformations since it is possible to write down the potential function for the flow which is obtained in this plane.

3 The Potential

The potential function Φ is required for the trailing vortex system (Fig.2) far behind the aerofoil moving downwards with velocity $v_{z\infty}$ in a stream which is undisturbed at infinity. It will be calculated as the sum of two parts:

(i) Φ_1. The potential function of a flow of velocity $-v_{z\infty}$ at infinity, streaming past the stationary form of the vortex sheet.

(ii) Φ_2. The potential function due to a uniform stream of velocity $v_{z\infty}$ everywhere. This second part is simply the superposition of a constant velocity onto the flow field (i) so that the vortex sheet is given its vertical velocity and the stream at infinity is brought to rest.

Φ_1 is calculable from the transformations of section 2, Φ_2 may be written down immediately.

Calculation of Φ_2

The potential function for a stream of velocity $v_{z\infty}$ parallel to the real axis in the ζ-plane is

$$\Phi_2 = \phi_2 + i\,\psi_2 = v_{z\infty}\,.\,\zeta \tag{21}$$

Calculation of Φ_1

In section 2 it is shown that in going from the ζ- to the ζ_6-plane the original boundary transforms into a straight line which is part of the y_6-axis whilst the point at infinity transforms into the point H_6 on the y_6-axis.

In the ζ-plane, the flow to be considered is a parallel one at infinity in the direction of the negative real axis and it will be shown that this transforms solely into the flow due to a doublet at H_6 with its axis coincident with the imaginary axis.

Consider the flow in the ζ-plane near $\zeta = \infty$; its potential function is

$$\Phi_1 = -\,v_{z\infty}\,\zeta\,. \tag{22}$$

In transforming to the ζ_3-plane via equations (1), (5) and (7)

$$\left|\frac{d\zeta}{d\zeta_3}\right|_{\zeta\to\infty} = s$$

so that

$$\Phi_1 = -\,v_{z\infty}\,.\,s\,.\,\zeta_3 \tag{23}$$

From equations (12), (14) and (16), near $\zeta_6 = \imath$ (i.e. H_6),

$$\zeta_3 = - \frac{H}{\left(\frac{\zeta_6}{\imath} - 1\right)} \tag{24}$$

where
$$H = \sqrt{\frac{4(4 + K_0^2)}{\left\{1 - \frac{1}{2}\left(\frac{g_1+1}{g_1-1}\right)^2\right\}}}$$

and hence

$$\Phi_1 = \phi_1 + i\,\psi_1 = \frac{v_{z\infty} \, . \, s \, . \, H}{\left(\frac{\zeta_6}{\imath} - 1\right)} \, . \tag{25}$$

This represents the flow due to a doublet situated at $\zeta_6 = \imath$ and directed along the y_6-axis.

In the ζ-plane the conditions to be satisfied were that there should be a parallel flow at infinity and that the shape of the cross-section of the trailing vortex system should be a streamline. The equation for this flow could not be written down immediately except for the region at infinity (equation (22)) and thus transformations were necessary. The state of affairs reached in the ζ_6-plane is a satisfactory one since the transformed boundary (part of the y_6-axis) is part of a streamline of the doublet flow. Thus it engenders no disturbances of the pure doublet flow and equation (25) which was derived for the region close to $\zeta_6 = \imath$ is valid for the whole of the ζ_6-plane.

The complete potential function is thus

$$\Phi = \Phi_1 + \Phi_2 = v_{z\infty}\left[\frac{s \, . \, H}{\left(\frac{\zeta_6}{\imath} - 1\right)} + \zeta\right] \tag{26}$$

and the velocity potential ϕ for points on the vortex surface $z_6 = 0$ is

$$\phi = v_{z\infty}\left[\frac{s \, . \, H}{y_6 - 1} + z\right] . \tag{27}$$

4 The Lift

4.1 Relationships between potential, lift and circulation

At any spanwise position on the wing-tank arrangement, the lift load* is given by

$$C_L(y)\ c(y) = \int_{-\infty}^{+\infty} (C_{p_{US}} - C_{p_{LS}})\ dx$$

and since

$$C_p \approx 2\frac{v_x}{V_o} = \frac{2}{V_o}\frac{\partial\phi}{\partial x}$$

then

$$C_L(y)\ c(y) = \frac{2}{V_o}\left[\underset{(x=\infty)}{\phi_{US}} - \underset{(x=\infty)}{\phi_{LS}}\right]$$

and the circulation is

$$\Gamma(y) = \frac{C_L(y)\ c(y)\ V_o}{2} = \underset{(x=\infty)}{\phi_{US}} - \underset{(x=\infty)}{\phi_{LS}} \qquad (28)$$

Thus the load distribution and circulation are related directly to the difference in potential between corresponding points on the upper and lower surfaces of the vortex system far downstream.

From equations (20), (27) and (28)

$$\frac{\Gamma(y)}{v_{z\infty}\cdot\frac{b}{2}} = \frac{2sH}{b}\left(\frac{y_6+1}{y_6-1}\right) + \frac{2}{b}\left(z_{US} - z_{LS}\right) \qquad (29)$$

so that the spanwise load distribution is calculable from the transformations in terms of $v_{z\infty}$, the rate of vertical descent of the vortex sheet, far downstream.

4.2 Determination of $v_{z\infty}$

In order to obtain the magnitude of the loads the value of $v_{z\infty}$ must be found. Nothing can be said about $v_{z\infty}$ from consideration of the flow

*In this report the tanks are assumed to be very long and attention is restricted to that part of their lift in the neighbourhood of the wing. In practice there are forces on the noses and tails of the tanks owing to the flow components across them; because of the downwash behind the wing and the presence of boundary layers the downloads on the tails, which exactly balance the uploads on the noses for isolated tanks in potential flow, are reduced, so that a net lift load results. This effect is discussed in connection with fuselages in Ref. 8 and equations (34) and (35) of that report may be used to estimate it. It must be remembered that those equations apply to one fuselage whilst in the present instance there are two tanks.

far downstream but it can be related to the induced incidence at the wing which may be determined from the boundary conditions on the wing.

$v_{z\infty}$ and the induced incidence α_i are related to each other by

$$\frac{v_{z\infty}}{V_o} = \frac{2}{\omega} \alpha_i \tag{30}$$

where ω is a 'downwash factor' varying from one for wings of very large aspect ratio to two for wings of very small aspect ratio.*

At the wing the effective incidence $\alpha_e(y)$ is composed of the geometrical incidence α, the induced incidence α_i, and an additional upwash incidence $\Delta\alpha_T(y)$ due to the tanks. This last additional incidence is produced by the flow component αV_o of the mainstream perpendicular to the axes of the tanks (see Fig.12) and is quite distinct from the influence which the tanks have on the trailing vortex system. Estimation of $\Delta\alpha_T(y)$ is dealt with in the Appendix.

The effective incidence is given by the relationship

$$\alpha_e(y) = \alpha + \Delta\alpha_T(y) - \alpha_i \tag{31}$$

and the local lift coefficient is

$$\begin{aligned} C_L(y) &= a(y)\ \alpha_e(y) \\ &= a(y)\ [\alpha + \Delta\alpha_T(y) - \alpha_i] \end{aligned} \tag{32}$$

where $a(y)$ is the sectional lift-curve slope. However, the circulation is already known from equation (29) and the local lift may also be expressed in terms of this:-

$$\begin{aligned} C_L(y) &= \frac{2\Gamma(y)}{V_o\ c(y)} \\ &= \frac{\Gamma(y)}{v_{z\infty} \cdot \frac{b}{2}} \cdot \frac{b}{c(y)} \cdot \frac{v_{z\infty}}{V_o} \end{aligned} \tag{33}$$

or, by equation (30)

$$= \frac{\Gamma(y)}{v_{z\infty} \cdot \frac{b}{2}} \cdot \frac{b}{c(y)} \cdot \frac{2}{\omega} \alpha_i . \tag{34}$$

Eliminating C_L from equations (32) and (34) gives an expression for the local chord

---

* Some discussion of ω will be found in section 6.1.

$$c(y) = \frac{2}{\omega} \cdot \frac{b}{a(y)} \cdot \frac{\dfrac{\Gamma(y)}{v_{Z\infty} \cdot \frac{b}{2}} \alpha_i}{[\alpha + \Delta\alpha_T(y) - \alpha_i]} \tag{35}$$

from which the particular minimum planforms implied by the method are calculable when α_i is known.

Integration of equation (35) leads to an implicit relationship for α_i in terms of known quantities; for by definition

$$\frac{1}{A} = \frac{2}{b^2} \int_0^{b/2} c(y) \, dy$$

whence from equation (35)

$$\frac{1}{A} = \frac{2}{\omega} \int_0^1 \frac{\dfrac{\Gamma(y)}{v_{Z\infty} \cdot \frac{b}{2}} \cdot \alpha_i \cdot d\left(\frac{2y}{b}\right)}{a(y) \; [\alpha + \Delta\alpha_T(y) - \alpha_i]} \tag{36}$$

In general this equation can be solved numerically for A in terms of α_i but since, in practice, A is known and α_i is required a process of successive approximation will be necessary and will involve considerable numerical computation. However for straight wings $a(y)$ is constant along the span and $\dfrac{\Gamma(y)}{v_{Z\infty} \cdot \frac{b}{2}}$ and $\Delta\alpha_T(y)$ are both functions of D/b so that a set of integrations can be made for $\frac{\omega a}{A}$ in terms of α_i/α and D/b only. From this a chart may be prepared relating α_i/α to D/b and $\frac{\omega a}{A}$; this has been done and appears as Fig.13.

The possibility of applying this chart generally is discussed in section 6.

4.3 Expressions for local and overall loads

Once α_i has been fixed in value, $\frac{v_{Z\infty}}{V_o}$ is given by $\frac{2}{\omega} \alpha_i$ and the local and overall loads are easily determined from equation (33) and its integrated forms. By equation (33),

$$C_L \, c = b \cdot \frac{v_{Z\infty}}{V_o} \cdot \frac{\Gamma}{v_{Z\infty} \cdot \frac{b}{2}} \tag{37}$$

and integrations over the wing semispan, the tank and the whole semi-span lead respectively to

$$
\left.
\begin{aligned}
\bar{C}_{L_W} &= A \cdot \frac{v_{Z\infty}}{V_o} \cdot J_W \\
\bar{C}_{L_T} &= A \cdot \frac{v_{Z\infty}}{V_o} \cdot J_T \\
\bar{C}_L &= A \cdot \frac{v_{Z\infty}}{V_o} \cdot J
\end{aligned}
\right\} \tag{38}
$$

where

$$
\left.
\begin{aligned}
J_W &= \int_0^1 \frac{\Gamma}{v_{Z\infty} \cdot \frac{b}{2}} \cdot d\left(\frac{2y}{b}\right) \\
J_T &= \int_1^{1+\frac{2D}{b}} \frac{\Gamma}{v_{Z\infty} \cdot \frac{b}{2}} \cdot d\left(\frac{2y}{b}\right) \\
J &= \int_0^{1+\frac{2D}{b}} \frac{\Gamma}{v_{Z\infty} \cdot \frac{b}{2}} \cdot d\left(\frac{2y}{b}\right)
\end{aligned}
\right\} \tag{39}
$$

For an isolated elliptical wing the value of J is $J_E = {}^{\pi}/2$.

Combining equation (37) with the first equation (38) gives the shape of the load distribution on the wing and tanks:

$$
\frac{C_L\, c}{\bar{C}_{L_W} \bar{c}} = \frac{1}{J_W} \frac{\Gamma}{v_{Z\infty} \cdot \frac{b}{2}} . \tag{40}
$$

Some examples of wing loads are given in Figs. 16 and 17, and of tank loads in Figs. 18 and 19.

Dividing the first two equations (38) gives the ratio of the loads on the tanks and on the wing

$$
\frac{\bar{C}_{L_T}}{\bar{C}_{L_W}} = \frac{J_T}{J_W} \tag{41}
$$

which is a function of ${}^{D}/b$ only and is shown in Fig.15.

The function J_W is shown in Fig.14; J_T and J are derivable from Figs. 14 and 15.

5 The Induced Drag

It is necessary only to consider the changes in vertical momentum and energy of the stream in passing from far upstream to far downstream of the wing. Assume that a cross sectional area S' of air is given a constant vertical velocity $v_{z\infty}$ far downstream (see p.190, reference 9); a mass of air $\rho_0 V_0 S'$ is influenced by the wing-tank arrangement every second and the equations of momentum and energy are

$$L = \rho_o V_o S' . v_{z\infty}$$

$$D_i V_o = \rho_o V_o S' . \tfrac{1}{2} v_{z\infty}^2$$

so that

$$\frac{\bar{C}_{D_i}}{\bar{C}_L} = \frac{D_i}{L} = \frac{v_{z\infty}}{2V_o} . \qquad (42)$$

In terms of lift coefficient $\bar{C}_L$, by equation (38)

$$\bar{C}_{D_i} = \frac{\bar{C}_L^{\,2}}{2 . A . J} . \qquad (43)$$

Since J for a wing with tanks is always greater than for the isolated wing, its induced drag at a given total lift is always smaller. For an isolated elliptic wing (which is not exactly the same as the isolated wing to give minimum induced drag in conjunction with tanks) $J_E = \pi/2$ and the expression $\frac{2AJ}{\pi}$ may be looked upon in some respects as an effective aspect ratio (this concept will be used later, see section 7).

6 The effects of low aspect ratio, non-minimum planforms and sweepback

6.1 Low aspect ratio

Theoretical work on wing loading has in the past been mostly confined to wings of large or very small aspect ratios, the downwash at the wing being taken in the one case equal to a half of that at infinity and in the other equal to the whole of it. The two have now been linked[10] by the concept of an induced incidence factor ω, varying from one to two, by D. Küchemann. In this way the usual equations relating lift, effective incidence, induced drag et cetera, which are derived under the assumptions of large aspect ratio, are enabled to retain the same form for the whole range of aspect ratio from zero to infinity. The expressions for ω and a will be found in section 7.

In connection with the present problem it will usually be true that the aspect ratio of the bound-vortex system on the tanks is much smaller than that on the wing, implying different values of ω. However, since equation (36) refers only to conditions on the wing, $v_{z\infty}$ will not depend on the value of ω for the tanks; furthermore, the loads on the wing and tank are dependent on $v_{z\infty}$ but not on ω (equation (38)) so that the aspect ratio of the tank does not enter into the minimum-induced-drag problem. This happy state of affairs is somewhat illusory, since some of the lift on the tanks is occurring further forwards than that on the wing so that its induced downwash has almost reached the full value at the wing; thus the assumption of constant induced velocity far downstream is incompatible with the assumption of constant induced velocity at the wing. In other words the shape of the vortex sheet (even neglecting any rolling up of the sheet) will change as it moves downstream. This effect would not be expected to cause large errors in the present application, and no attempt is made to take it into account.

6.2 Non-minimum planforms

If comparisons are made between the local lift coefficients and the load distributions of isolated plain wings, it is found that the former vary widely between wings of differing planforms whilst the latter are never far from being elliptical - the load distribution for minimum induced drag. Hence in applying the present results to non-minimum planforms, it might be expected that the additional loads due to the tanks will apply with fair accuracy, but not so the additional lift coefficients.

The particular planforms to which the calculations apply are given by

$$\frac{c}{\bar{c}} = \frac{\dfrac{C_L\, c}{\alpha\, \bar{c}}}{a\left[1 + \dfrac{\Delta\alpha_T}{\alpha} - \dfrac{\alpha_i}{\alpha}\right]} , \qquad (44)$$

which is another form of equation (35). The loads on these wings without tanks may be obtained by the normal methods (e.g. by Ref.11), or if less accuracy may be tolerated the load distribution on an elliptic wing may be assumed. Some light on such an approximation will be shed by the worked example in the next section.

6.3 Sweepback

The dominant effect of sweepback is[9] to cause increases in the sectional lift curve slope near to the tips and decreases in it over the rest of the wing, especially near to the centre.

Local values of a could be introduced into equation (36) - values appropriate to the real wing being considered - and the equation solved by an iteration process for each particular example. Such a procedure is tedious and should be avoided if possible so it is proposed that a mean value of a be used* (for large aspect ratio this is taken as $a_0 \cos \phi$), in which case the results in Fig.13 still apply. This approximation implies a change in α_i and hence in the level of the loads on the wing-tank arrangement, but no change in the shape of the load distribution (equation (40) is independent of a). Since, however, a different basic wing is implied (equation (44)) these statements do not necessarily apply to the additional loads.

To obtain some idea of the magnitudes involved in the approximation some calculations have been made relevant to a straight tapered wing of 59° sweepback and aspect ratio 3.61 (this is the wing of the worked example in reference 11) with tip-tanks of diameter 0.15x semi-span.

Span loadings have been calculated for minimum wing-tank configurations [$2D/b = 0.15$, $A = 3.61$] under the assumptions of (i) a mean value of a and (ii) local values of a as for the real wing. They have also been obtained for the isolated wings implied by the minimum induced-drag condition.

Fig.20 shows the results for constant a. The planform assumed is not far from being elliptical, nor is its loading.

---

*The same approximation in connection with swept wings with endplates[12] gives satisfactory agreement with experimental results.

Fig.21 shows the results with varying a. The planform is almost elliptical except over the inboard 40% of the semi-span and the load distribution on this wing alone is close to that on the real wing (i.e. the straight tapered wing). The value of α_1 obtained from equation (36) using local a values is 10% less than when a is kept constant. However, the same is roughly true for the implied isolated wings and from Fig.22 it is seen that the differences between the additional loads calculated by the two methods are very small.

For comparison, there is included in Fig.22 the difference in load between the minimum arrangement for constant a and the corresponding isolated elliptical wing. The order of accuracy given by this very swift approximate method may be sufficient for most applications; the errors involved will of course decrease with tank size.

Fig.23 shows the local loads and lift coefficients on the real wing and on the real wing with tanks The additional loads have been taken from the a = constant calculation.

The conclusions to be drawn from the example are:-

(a) it will be sufficiently accurate in practice to use a mean value of the sectional lift-curve slope, and

(b) it may be necessary, where large tanks are concerned, to work out the loading on the wing alone implied by the calculations in order to obtain accurate estimates of the distribution of the additional load.

Some of the numerical work involved in the example will be found in Table I.

7 Calculation Procedure

The method of calculation will be outlined for examples in which it is assumed to be sufficiently accurate to take an elliptical wing alone as datum. (see section 6 for a discussion of the accuracy in doing this); some numerical results for such an example are given in Table I.

In any particular application the known quantities are wing aspect ratio A, the mean sweepback of the half-chord line φ, the thickness-chord ratio t/c and the tank diameter as a fraction of the wing semi-span $2D/b$.

In order to determine $-\alpha_1/\alpha$ from Fig.13, the parameter $\frac{\omega a}{2\pi A}$ must be calculated, for which purposes the following expressions* of D. Küchemann may be used:

$$\omega = 2n = 2 - \frac{1}{\left\{1 + \left(\frac{a_0 \cos \varphi_e}{\pi A_e}\right)^2\right\}^{\frac{1}{4\left(1 + \frac{\varphi_e}{\pi/2}\right)}}} \tag{45}$$

$$a = \frac{2a_0 n \cos \varphi_e}{1 - \pi n \cot \pi n} \tag{46}$$

*These will appear shortly in Ref.10.

where

$$\varphi_e = \frac{\varphi}{\sqrt[4]{1 + \left(\frac{a_o \cos \varphi}{\pi A_e}\right)^2}} . \tag{47}$$

In these expressions a_o is a sectional lift curve slope given by

$$a_o = K.\, 2\pi \left[1 + 0.8 \frac{t/c}{\cos \varphi}\right] \tag{48}$$

where K is a factor depending on Reynolds number, equal to about 0.92 for $R = 2 \times 10^6$ and equal to 1.00 for non-viscous flow. The equations also include an effective aspect ratio A_e which is introduced from the phsyical reasoning that ω and a are dependent on the distribution of vorticity over the wing and tanks rather than the geometrical aspect ratio of the wing. A_e is taken arbitrarily the same as the effective aspect ratio to give the correct induced drag (see section 5), that is

$$\frac{A_e}{A} = \frac{J}{J_E} = \frac{2J_W}{\pi}\left[1 + \frac{\bar{C}_{L_T}}{\bar{C}_{L_W}}\right] . \tag{49}$$

Owing to the different effective aspect ratios of the wing with tanks and the isolated elliptical wings, it is necessary to derive values of $\frac{\omega\, a}{2\pi A}$ for both of them (see Table I).

Values of $^{\alpha_i}/\alpha$ are read from Fig.13 and $\frac{1}{\alpha}\frac{v_{z\infty}}{V_o}$ calculated from equation (30).

Overall lift coefficients on the wing with tanks and the wing alone are given by equations (38).

The mean lift coefficient on the tanks is obtained from that on the wing and the value of $\frac{\bar{C}_{L_T}}{\bar{C}_{L_W}}$ read from Fig.15. [N.B. $\bar{C}_{L_T}$ and all mean lift coefficients are made non-dimensional with the wing area.]

The distributions of the loads on the wing and tanks are obtainable in the form $\frac{C_L\, c}{\bar{C}_{L_W} \bar{c}}$ and $\frac{C_L\, c}{(C_L\, c)_{J}}$ from Figs. 17 and 19 respectively and these may be compared with the values for the isolated elliptic wing after conversion into coefficients of the form $\frac{C_L\, c}{\alpha\, \bar{c}}$ by appropriate multiplications.

Thus the additional loads due to tanks are given by

$$\Delta \frac{C_L\, c}{\alpha\, \bar{c}} = \frac{C_L\, c}{\alpha \bar{c}} - \left(\frac{C_L\, c}{\alpha\, \bar{c}}\right)_E \tag{49}$$

which may be added to the load distribution on the actual wing alone, estimated by one of the usual methods (e.g. by Ref.10). Local lift coefficients are finally derived by dividing the load coefficients by the $c/\bar{c}$ values of the real wing.

8 Further Work

The first three transformations of section 2 together with W. Mangler's transformations[5] for wings with inboard endplates could be used to obtain span loadings on wings with nacelles.

REFERENCES

No.	Author	Title, etc.
1	M.M. Munk	Isoperimetrische Aufgaben aus der Theorie des Fluges. Diss. Gottingen (1918).
2	L. Prandtl	Tragflügeltheorie I and II.
3	E. Trefftz	Prandtlsche Tragflächen - und Propeller - theorie. Z.a.M.M. Vol.1, p.206 (1921).
4	W. Mangler	The distribution of lift over an aerofoil with endplates. ARC Report No. 3414 (1938).
5	W. Mangler	Lift distribution around aerofoils with endplates. R.T.P. Translation No. 2338.
6	I.E. Garrick	Potential flow about arbitrary biplane wing sections. NACA Report No. 542 (1936).
7	J. Weber	Theoretical load distributions on a wing with a cylindrical body at one end. RAE Report No. Aero 2467. ARC No. 15,232.
8	J. Weber D.A. Kirby D.J. Kettle	An extension of Multhopp's method of calculating the spanwise loading of wing fuselage combinations. RAE Report No. Aero 2446. ARC No. 14,830.
9	L. Prandtl O.G. Tietgens	Applied hydro- and aero-mechanics.
10	D. Küchemann	A simple method for calculating the span and chordwise loading on straight unswept wings of any given aspect ratio at subsonic speeds. RAE Report No. Aero 2476 (1952). ARC No. 15,633.
11	D. Küchemann	A simple method of calculating the span and chordwise loading on thin swept wings. ARC No. 13,758. August 1950.
12	D. Küchemann D.J. Kettle	The effect of endplates on swept wings. C.P. 104. June 1951.

APPENDIX

Estimation of $\Delta\alpha_T$

The tank upwash incidence α_T can only be conveniently calculated for circular cylindrical tanks which extend a long way ahead and behind of the wing and this is the only case which will be considered. Since in practice these conditions will not generally be fulfilled, the estimated loads may be too large. At the same time, there are reasons to believe that a very short length of cylinder is sufficient to give local two-dimensional conditions close to the surface, where the effects are most intense, and so the errors involved may not be great.

Assuming the tanks have no incidence relative to the wing, which is inclined at an angle α to the mainstream, there will be a velocity component αV_o perpendicular to the axes of the tanks, giving rise to increased vertical velocities in the plane containing the wing, especially near to the tank-wing junctions (Fig.12). The distribution of this velocity may be estimated from the two-dimensional flow of a parallel stream at infinity past two circles, the undisturbed stream direction being perpendicular to the line of centres of the circles. The problem is that of finding the velocity distribution along AB in Fig.4 when AB is no longer a solid boundary. Transformations as far as the ζ_3-plane only need be considered, where the circles have become straight lines coincident with streamlines.

Along AB, $z = 0$, $z_2 = \pi$ and in transforming to the ζ_3-plane a velocity αV_o at infinity in the physical plane becomes a velocity $s.\alpha.V_o$. Hence it may be shown that the velocity along AB is given by

$$v_z = -\alpha V_o\left(1 + \frac{\alpha_T}{\alpha}\right) = \frac{dW}{d\zeta_3}\cdot\frac{d\zeta_3}{d\zeta_2}\cdot\frac{d\zeta_2}{d\zeta} \qquad (A1)$$

where

$$W = -s.\alpha V_o\,\zeta_3 \qquad (A2)$$

$$\frac{d\zeta_2}{d\zeta} = \frac{2s}{s^2 - y^2} \qquad (A3)$$

and

$$\frac{d\zeta_3}{d\zeta_2} = \frac{1}{1 + \cosh y_2} + \frac{1}{1 + \cosh\,(y_2 + 2\beta)}$$

$$- 4\sum_{\ell=1}^{\ell=\infty}\sum_{m=1}^{m=\infty} m(-1)^m\, e^{-4\beta\ell m}\left\{\cosh y_2 + \cosh\,(y_2 + 2\beta)\right\}. \qquad (A4)$$

Alternatively, since the tanks are far apart compared with their diameters, an approximate estimate may be made by simply adding the velocities at any given point due to each cylinder separately. The expression for α_T is then

$$\frac{\Delta\alpha_T}{\alpha} = \left(\frac{D}{b}\right)^2 \left[\frac{1}{\left(1 + \frac{2y}{b} + \frac{D}{b}\right)^2} + \frac{1}{\left(1 - \frac{2y}{b} + \frac{D}{b}\right)^2}\right] \qquad \text{(A5)}$$

and for tanks of the size considered in this report, the approximation is extremely good (Fig.12).

TABLE I

Specimen calculation

Data: $A = 3.61$, $\varphi = 55^\circ$, $^{2D}/_b = 0.15$
$^t/_c = 0.14$, $R = 2 \times 10^6$.

Calculations:

	Elliptic wing alone	Wing with tanks
Fig.14	$J_E = 1.571$	$J_W = 2.16$
Fig.15		$\dfrac{\bar{C}_{L_T}}{\bar{C}_{L_W}} = 0.067$
Eqn. (49)		$A_e = 5.30$
Eqn. (48)	$a_o = 2\pi \times 1.15$	$2\pi \times 1.15$
Eqn. (47)	$\varphi_e = 53.3^\circ$	54.1°
Eqn. (45)	$\omega = 1.021$	1.011
Eqn. (46)	$a = 4.19$	4.17
Fig.13	$\dfrac{\omega a}{2\pi A} = 0.189$	0.186
	$\dfrac{\alpha_1}{\alpha} = 0.275$	0.222

Overall loads

Eqns. (30),(38)	$\dfrac{\bar{C}_{L_E}}{\alpha} = 3.05$	$\dfrac{\bar{C}_{L_W}}{\alpha} = 3.42$
		$\dfrac{\bar{C}_{L_T}}{\alpha} = 0.23$
		$\dfrac{\bar{C}_L}{\alpha} = 3.65^*$

$\dfrac{\text{Lift on wing and tanks}}{\text{Lift on wing alone}} \div \dfrac{\bar{C}_L}{\bar{C}_{L_E}} = 1.195^{**}$

Extra lift due to tanks $\div \dfrac{\bar{C}_L}{\alpha} - \dfrac{\bar{C}_{L_E}}{\alpha} = 0.60$

* Lift due to nose and tail effects is not included, see section 4.1

** Correct to nearest 0.005.

TABLE I (Contd)

Distribution of Extra Load due to Tanks

$2y/b$	Elliptical Wing (1) $\frac{C_L c}{\bar{C}_L \bar{c}}$	(2) $\frac{C_L c}{\alpha \bar{c}} = 3.05$ (1)	(3) $\frac{C_L c}{\bar{C}_{L_W} \bar{c}}$	Wing with tanks (4) $\frac{C_L c}{\alpha \bar{c}} = 3.42$ (3)	(5) $\Delta \frac{C_L c}{\alpha \bar{c}}$ = (4) - (2)
0	1.273	3.88	1.137	3.89	0.01
0.2	1.247	3.80	1.119	3.83	0.03
0.4	1.167	3.56	1.072	3.66	0.10
0.6	1.018	3.07	0.991	3.39	0.32
0.8	0.764	2.33	0.875	2.99	0.66
0.9	0.555	1.69	0.798	2.73	1.04
0.95	0.398	1.22	0.768	2.63	1.41
1.00	0	0	0.741	2.53	2.53
$\frac{y - b/2}{D/2}$					
0.100	-	-	0.669	2.29	2.29
0.233	-	-	0.597	2.04	2.04
0.367	-	-	0.534	1.83	1.83
0.500	-	-	0.475	1.62	1.62
0.667	-	-	0.380	1.30	1.30
0.833	-	-	0.267	0.91	0.91
0.900	-	-	0.203	0.69	0.69
1.00	-	-	0	0	0

Columns (1) and (3) are obtained from Figs. 17 and 19.

Wt.2078. CP147.K3. Printed in Great Britain.

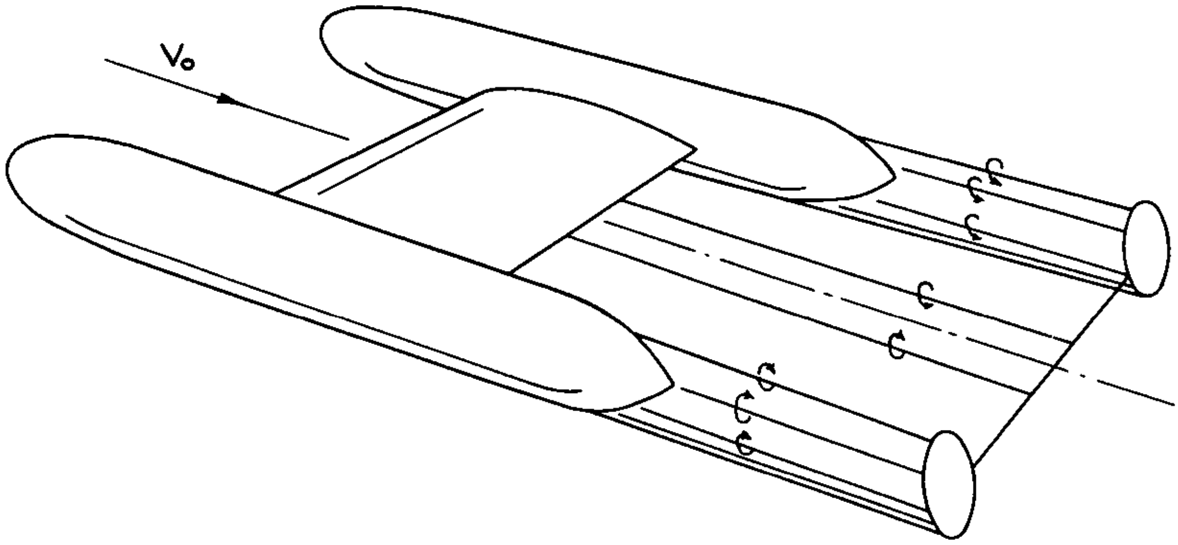

FIG. 1 WING WITH TIP-TANKS AND THE DOWNSTREAM VORTEX SURFACE.

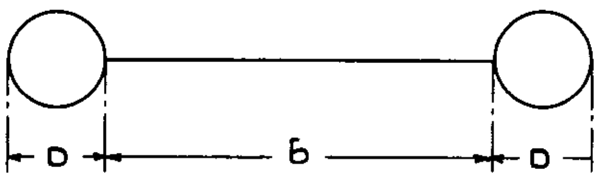

FIG. 2 SECTION THROUGH THE VORTEX SURFACE

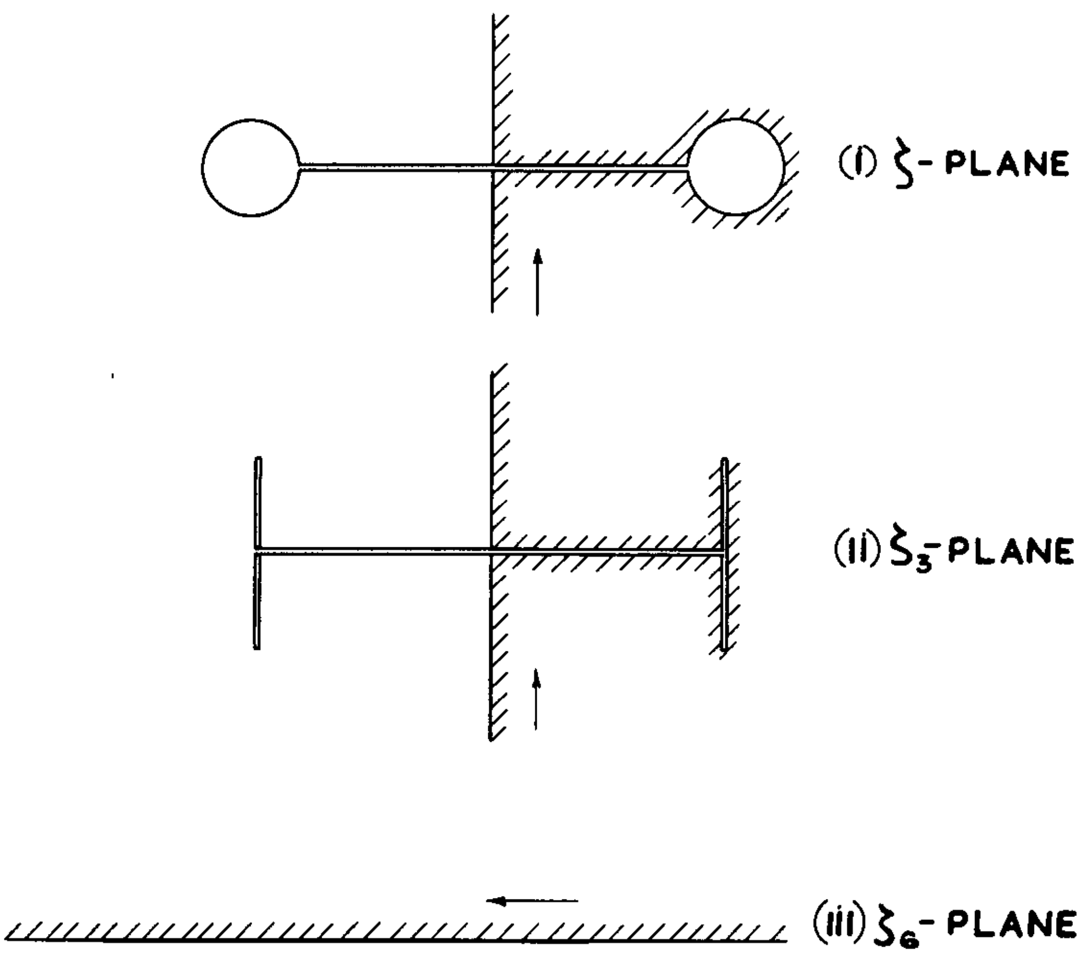

FIG. 3 PRINCIPAL STAGES IN THE CONFORMAL TRANSFORMATIONS.

FIG. 4,5,6&7

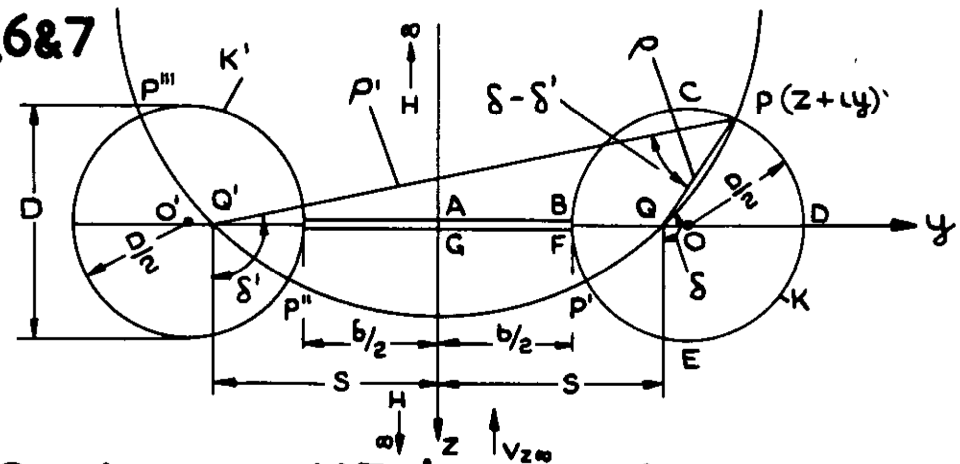

FIG. 4 THE ζ - PLANE.

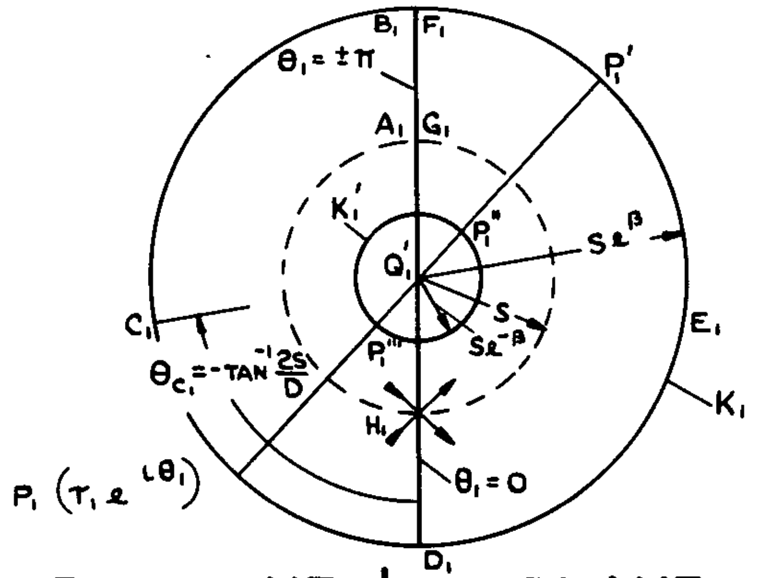

FIG. 5 THE ζ_1 - PLANE.

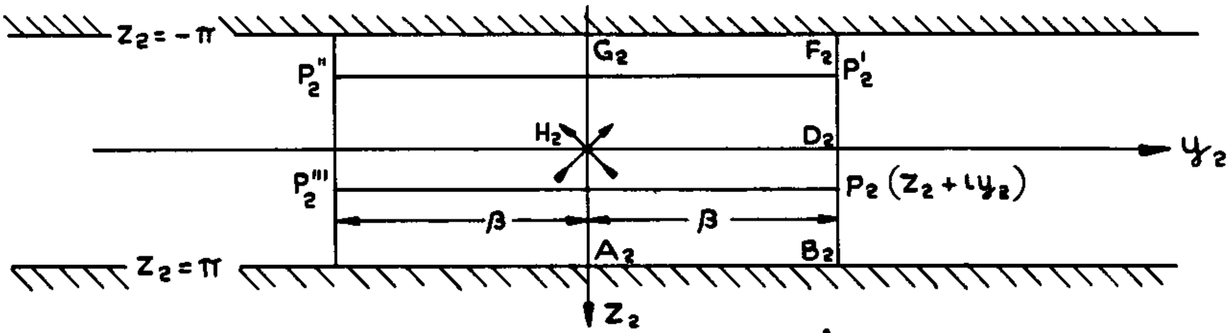

FIG.6 A STRIP OF THE ζ_2 - PLANE.

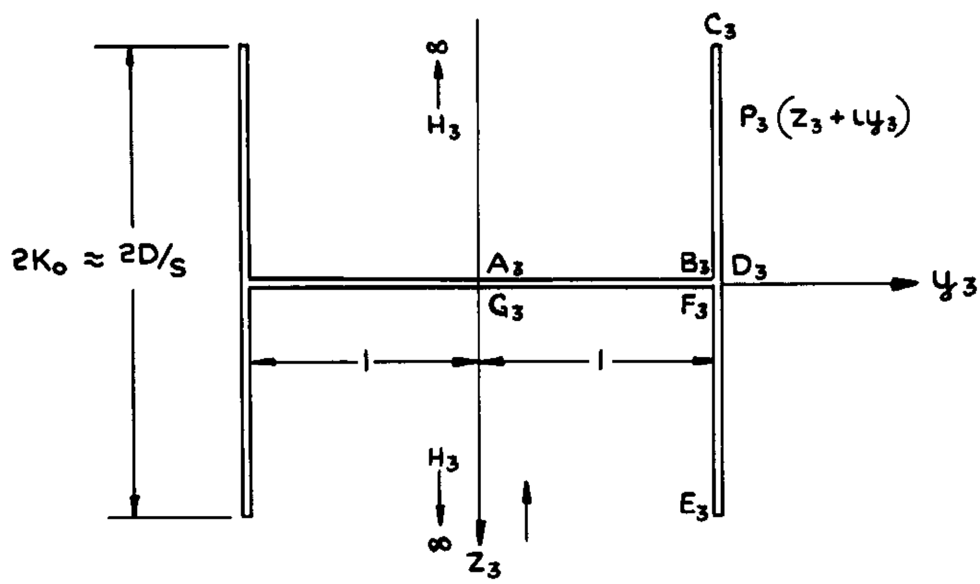

FIG.7 THE ζ_3 - PLANE.

FIG. 8. 9. 10 & 11

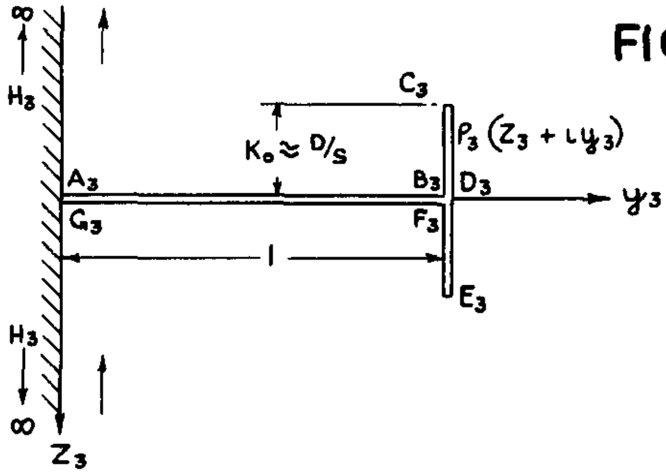

FIG. 8 HALF OF THE ζ_3-PLANE

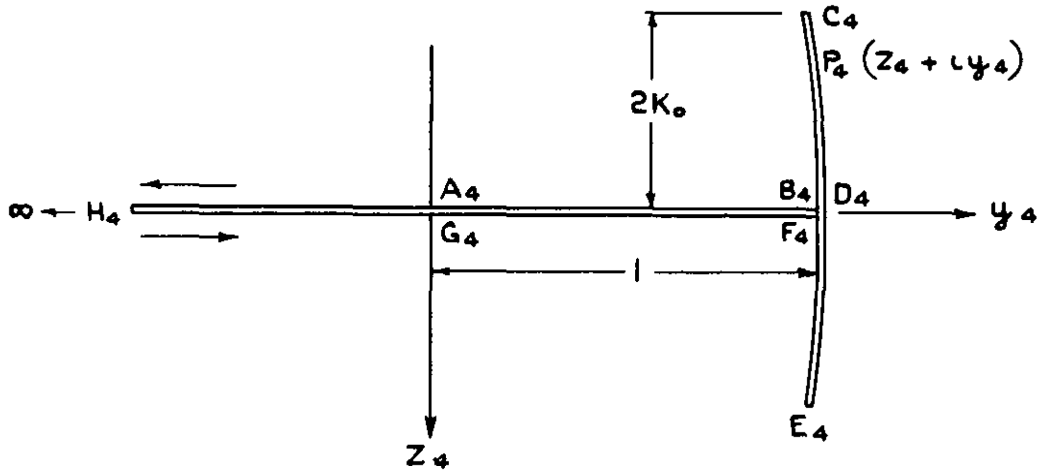

FIG. 9 THE ζ_4-PLANE

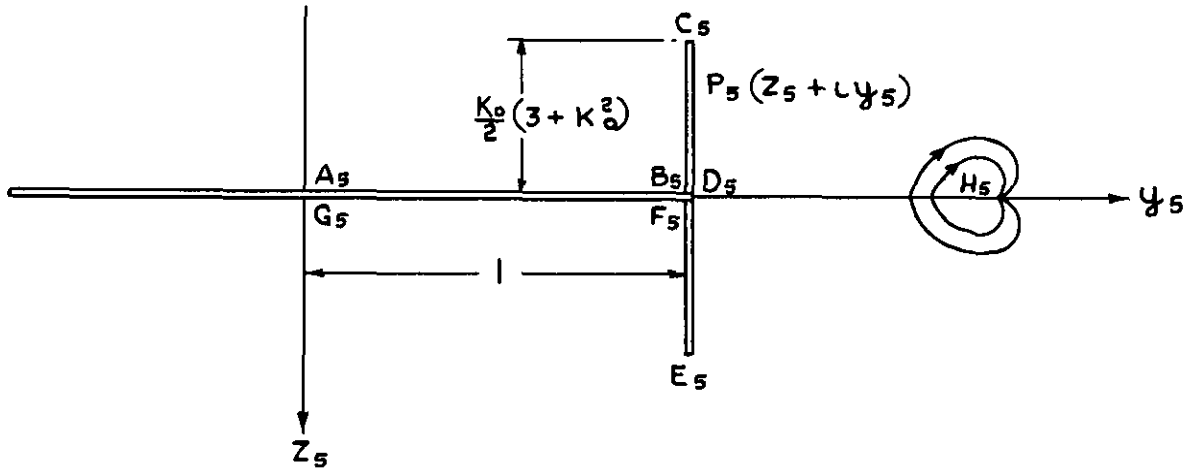

FIG. 10 THE ζ_5-PLANE

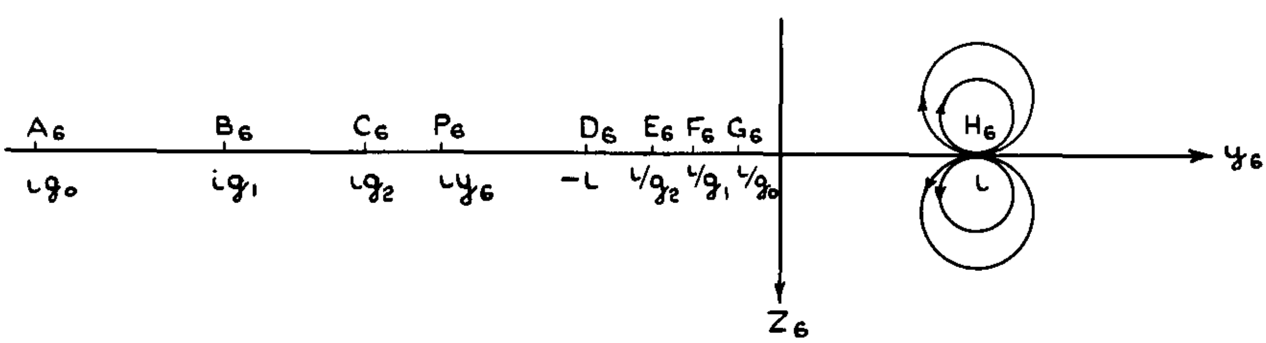

FIG. 11 THE ζ_6-PLANE

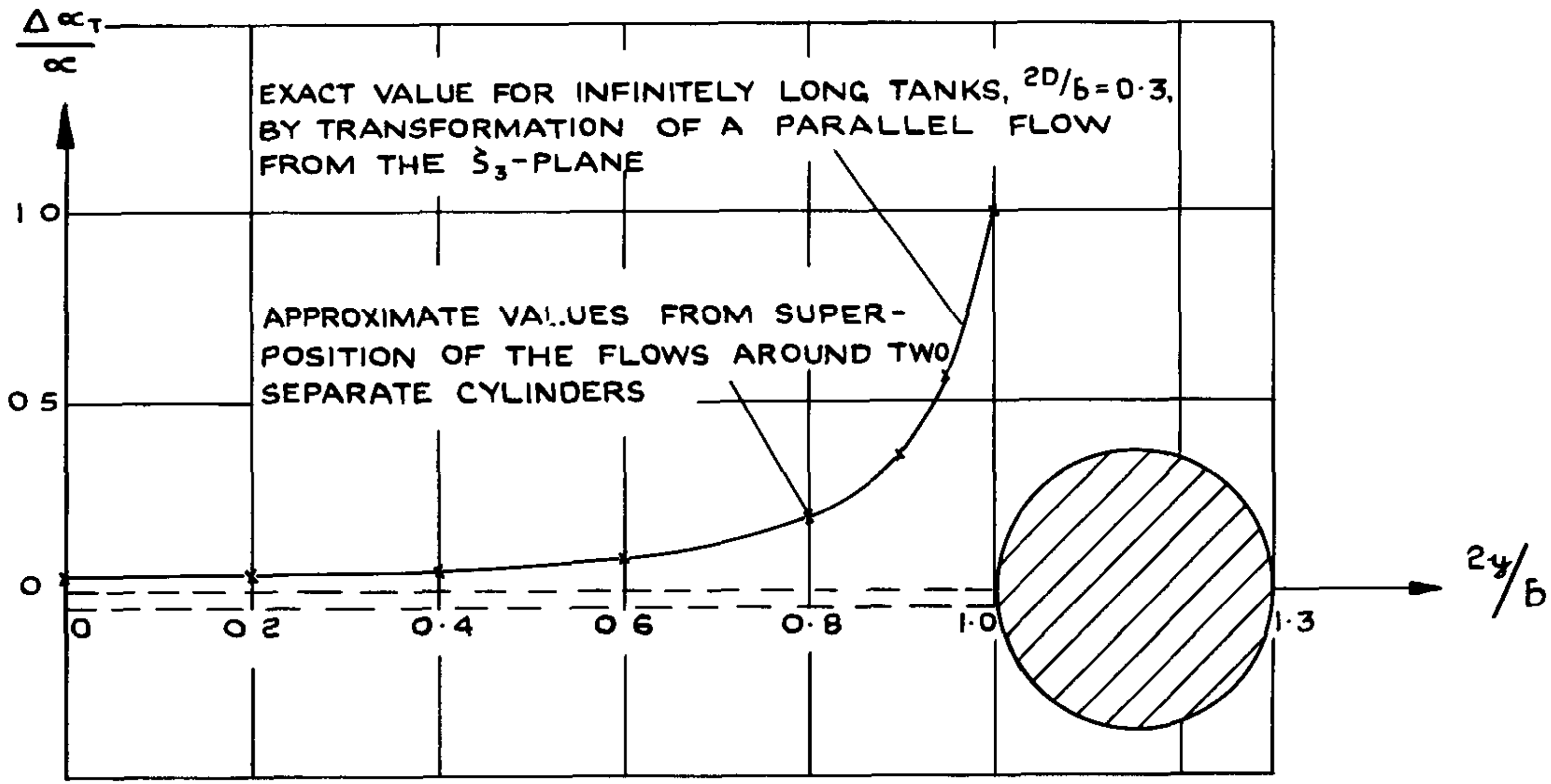

FIG.12 THE ADDITIONAL INCIDENCE $\Delta\alpha_T$ DUE TO FLOW AROUND THE TANKS.

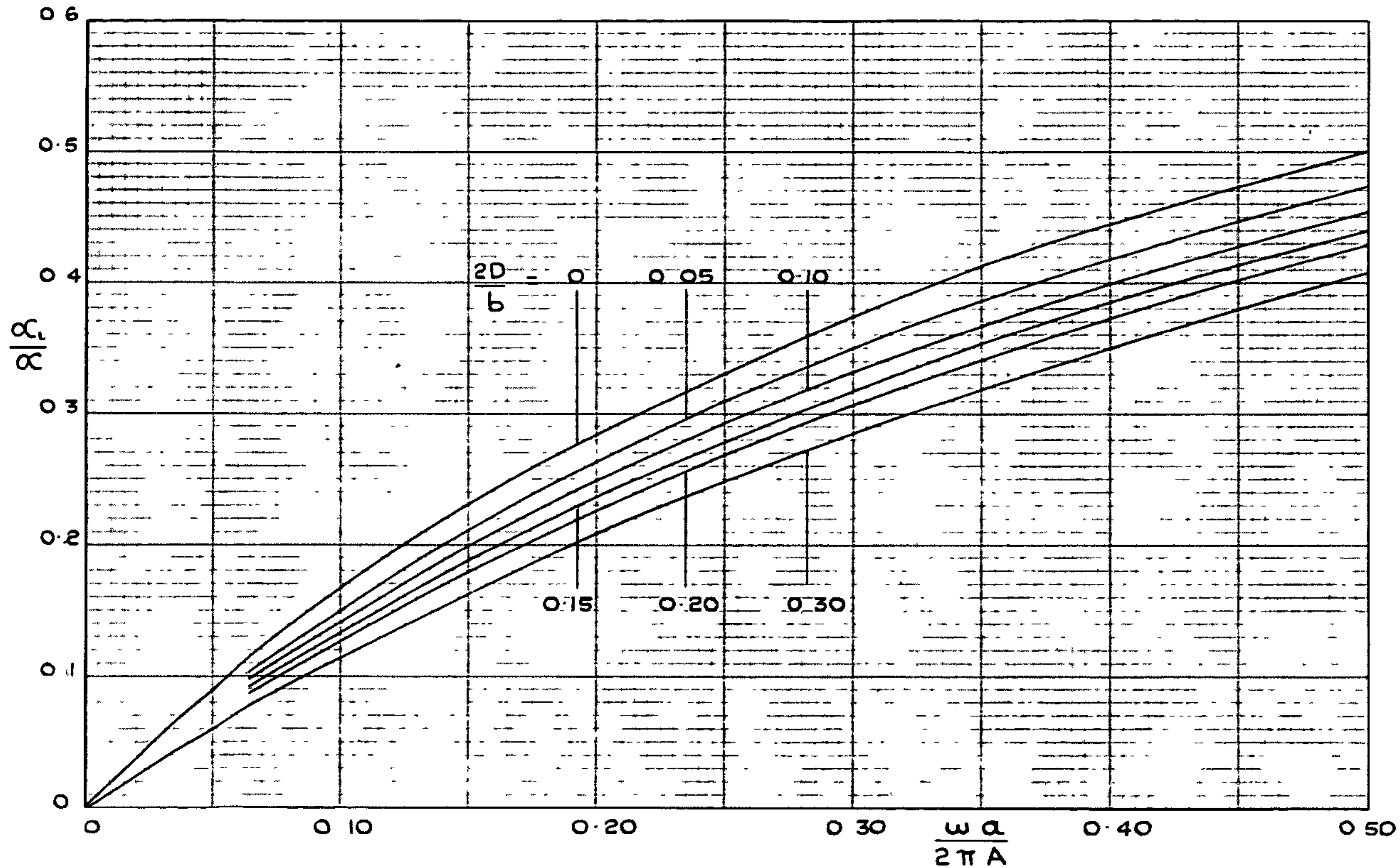

FIG. 13. CHART FOR DETERMINATION OF INDUCED INCIDENCE.

FIG. 13.

FIG.14.

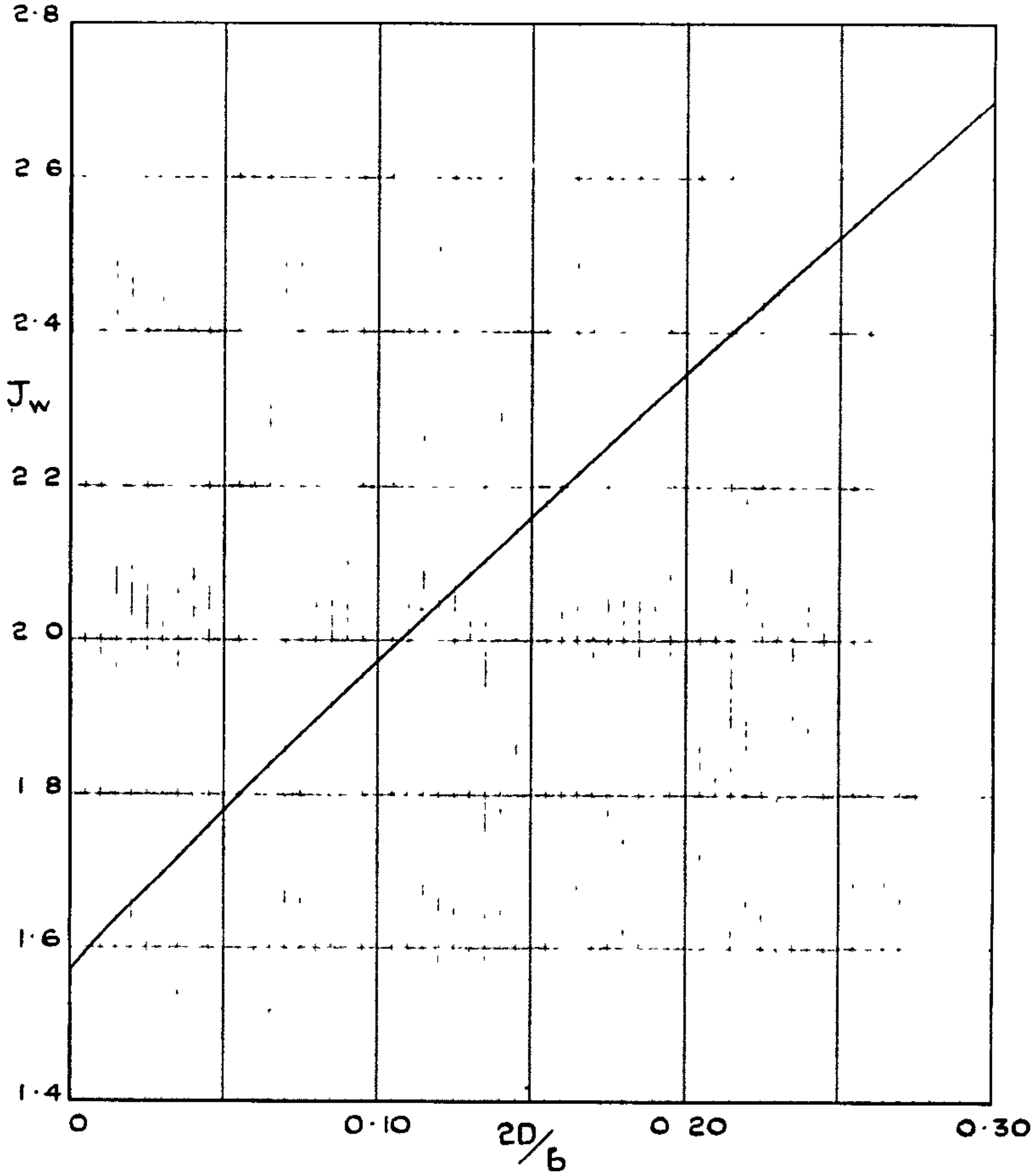

FIG.14. THE FUNCTION J_W REQUIRED IN THE ESTIMATION OF TOTAL WING LOAD.

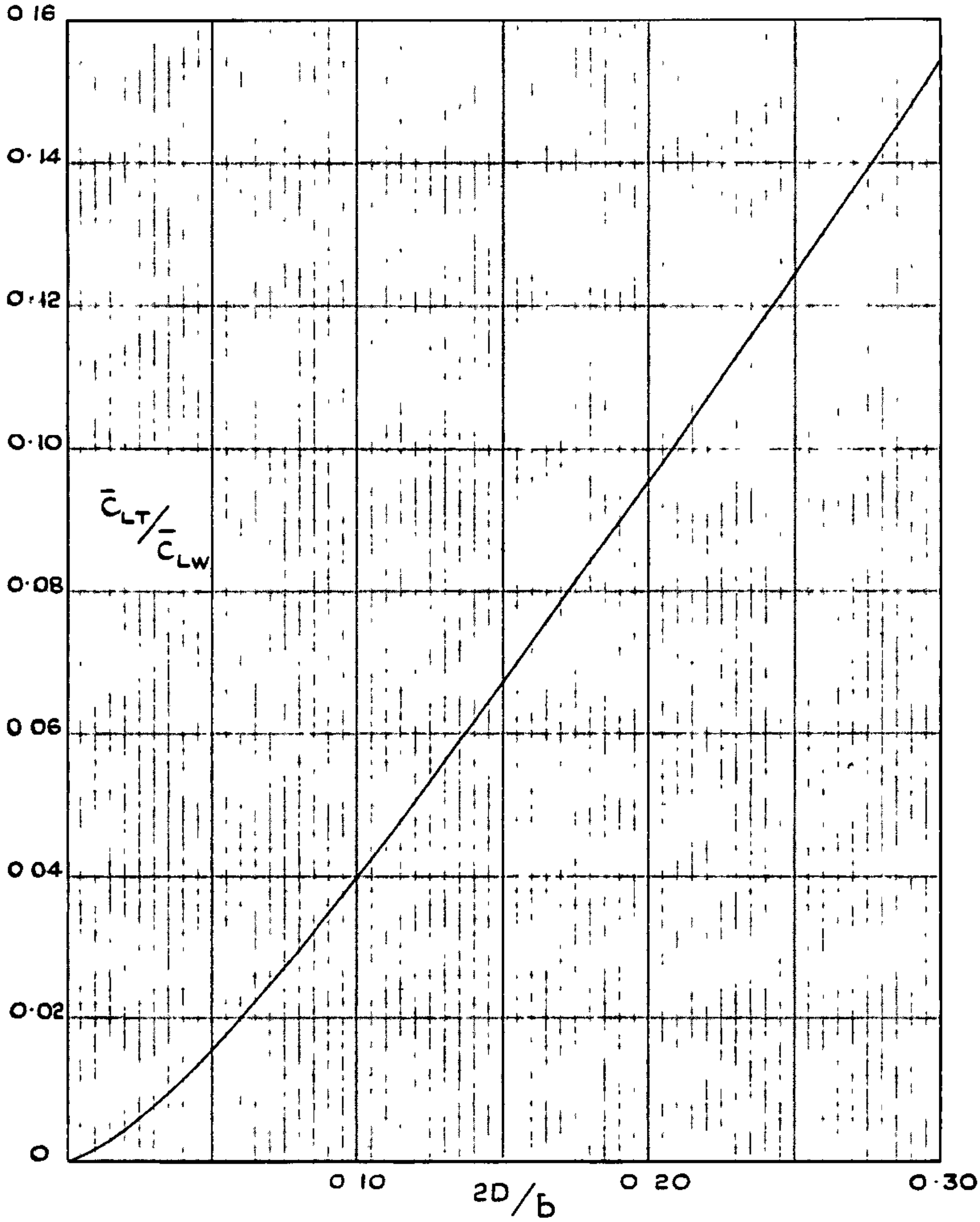

FIG.15. RATIO OF LOADS ON TANK & WING.

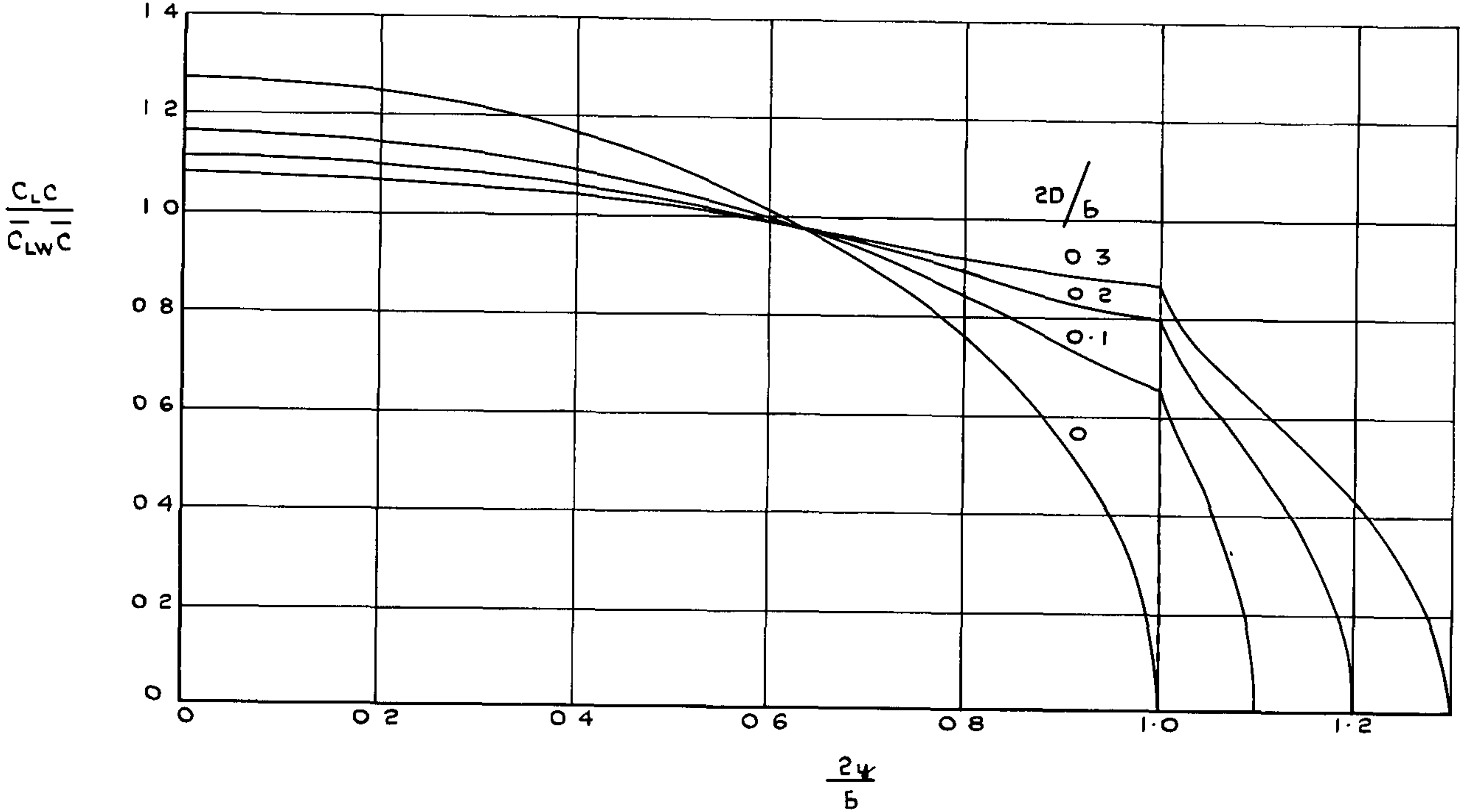

FIG. 16 SOME SPANWISE LOAD DISTRIBUTIONS ON THE WING WITH TANKS.

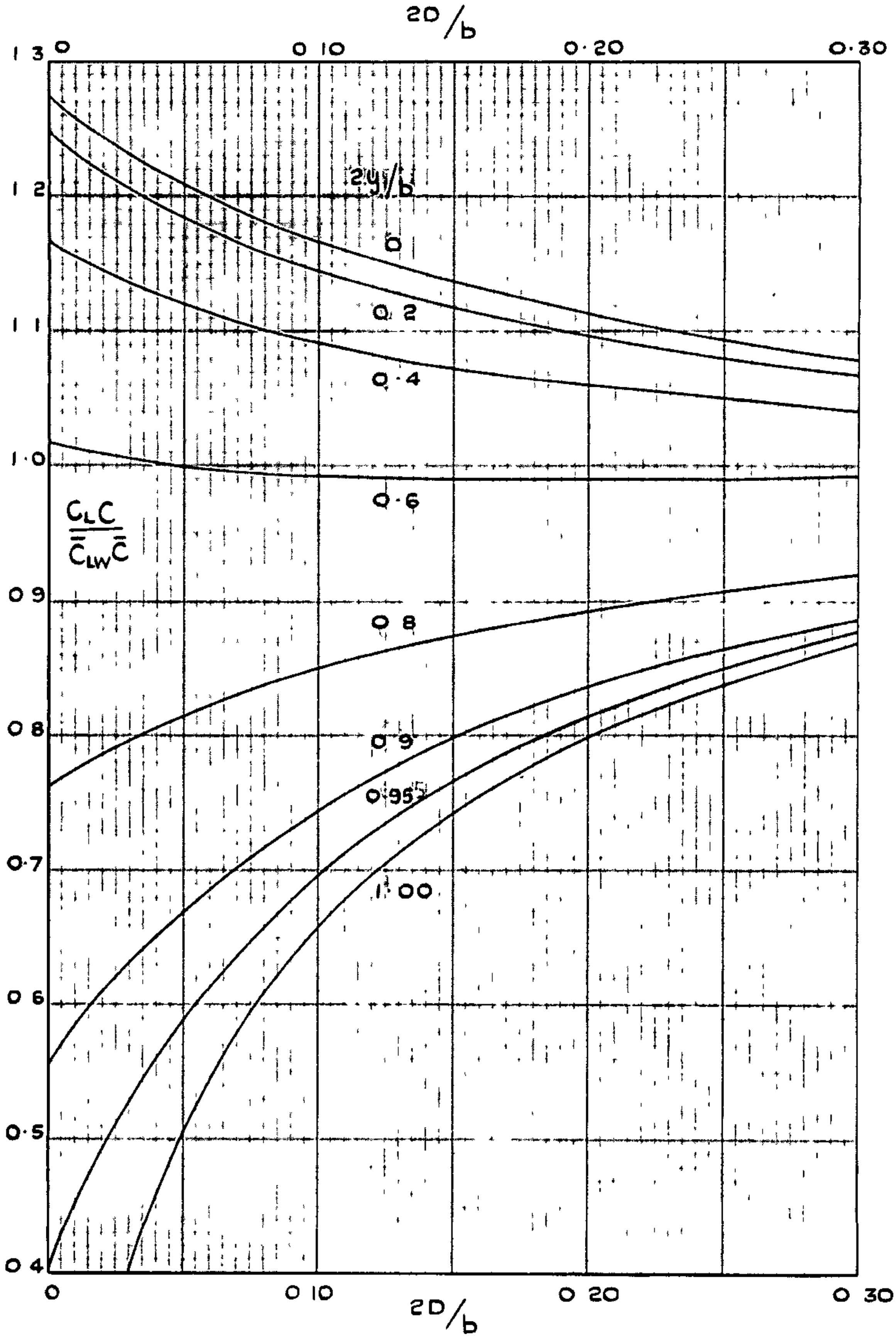

FIG. 17. INTERPOLATION CURVES FOR DETERMINING THE SPANWISE WING LOADING.

FIG. 18 & 19.

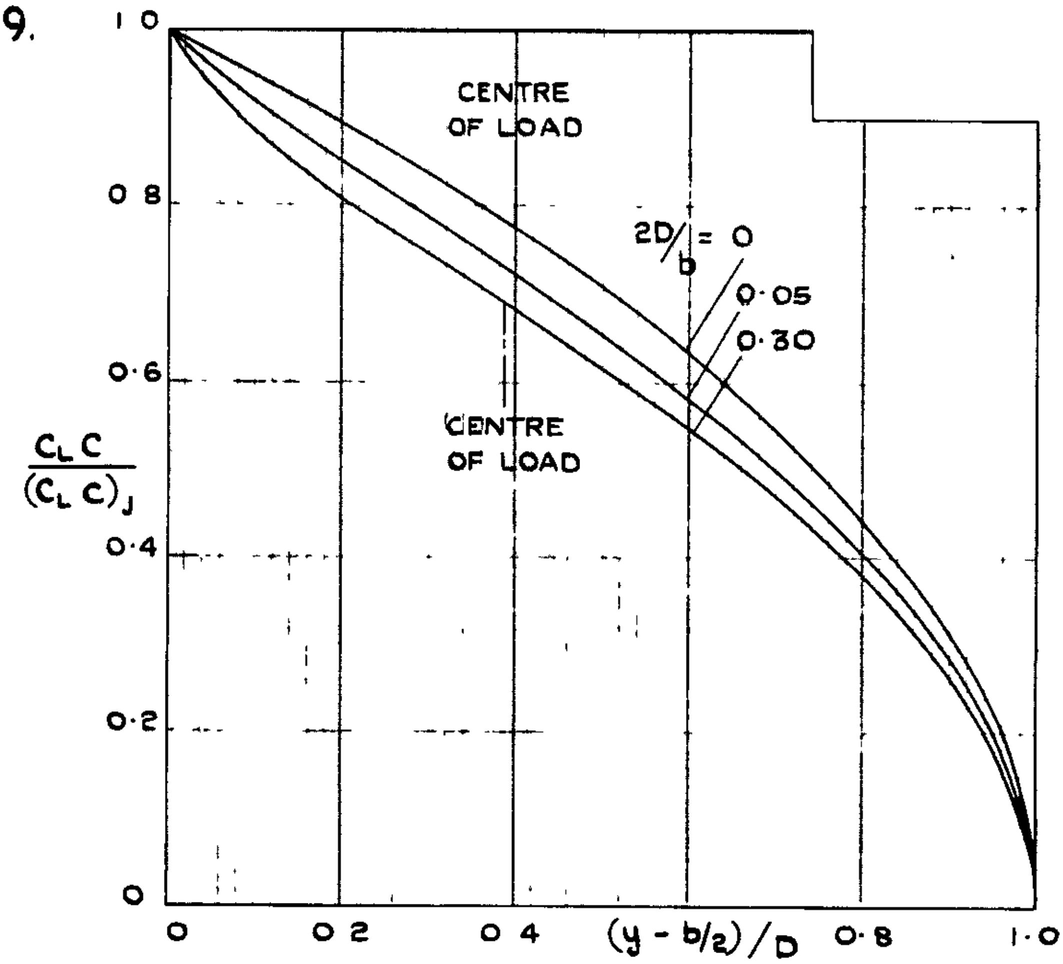

FIG. 18. SOME SPANWISE LOAD DISTRIBUTIONS ON THE TANKS.

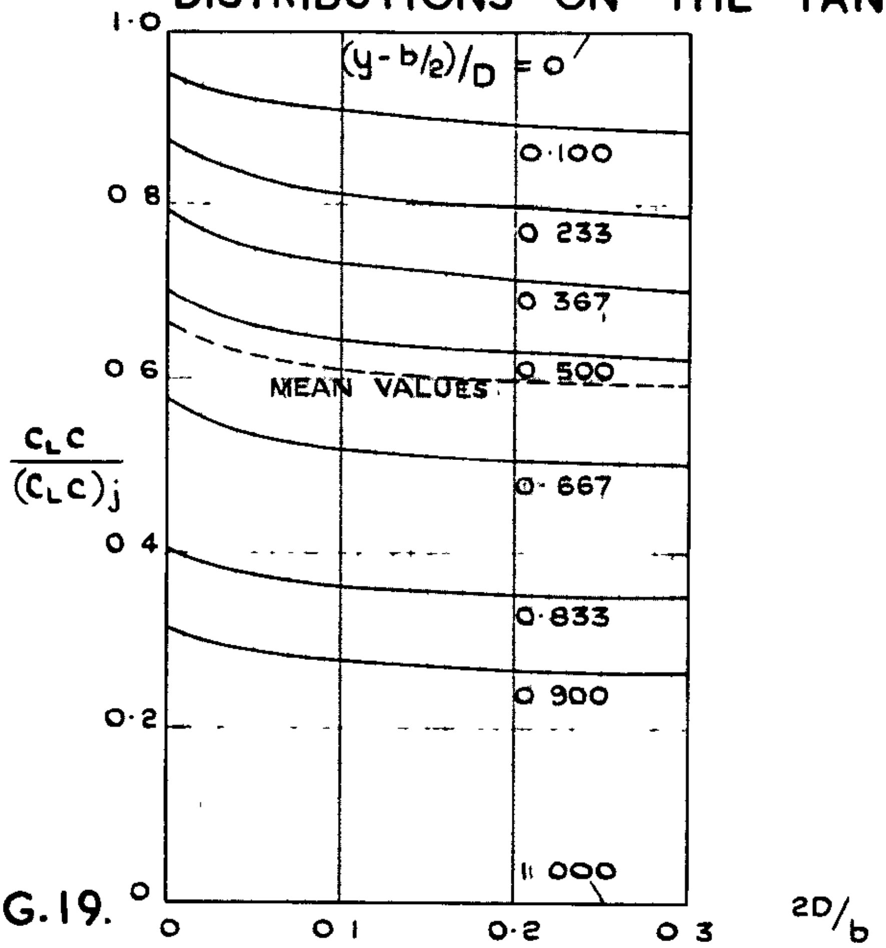

FIG. 19. INTERPOLATION CURVES FOR DETERMINING THE SPANWISE LOAD DISTRIBUTION ON THE TANKS.

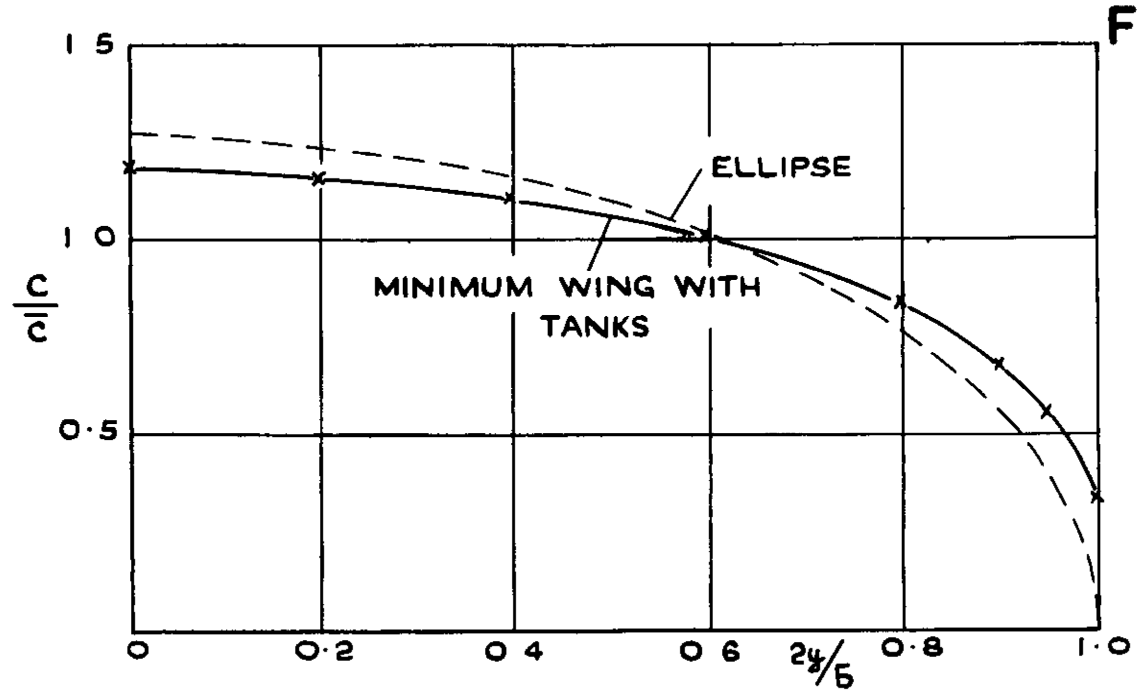

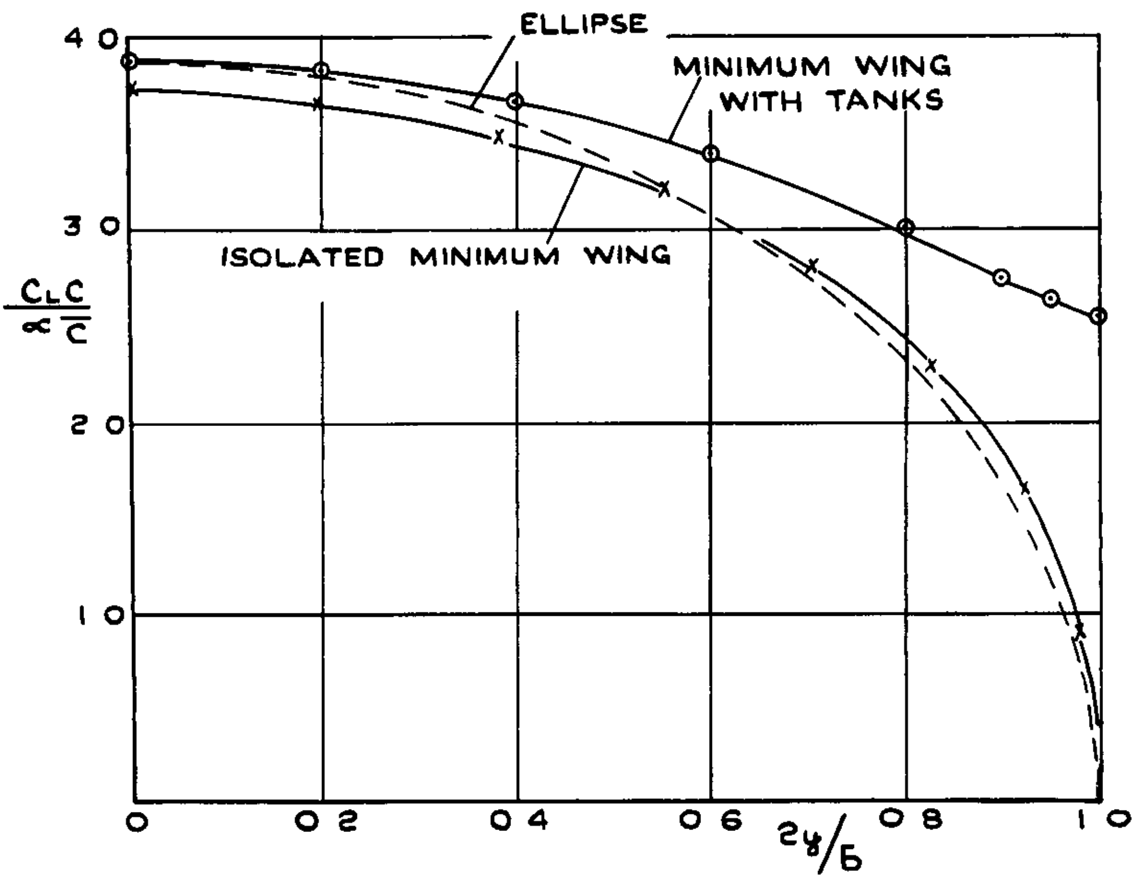

FIG. 20. PLANFORMS AND WING LOADINGS FOR A 59° SWEPT WING, A = 3·61, WITH TANKS $2D/b$ = 0·15, BY AN APPROXIMATE METHOD UTILISING A CONSTANT VALUE ALONG SPAN OF THE SECTION LIFT-CURVE SLOPE, 'a'.

FIG. 21

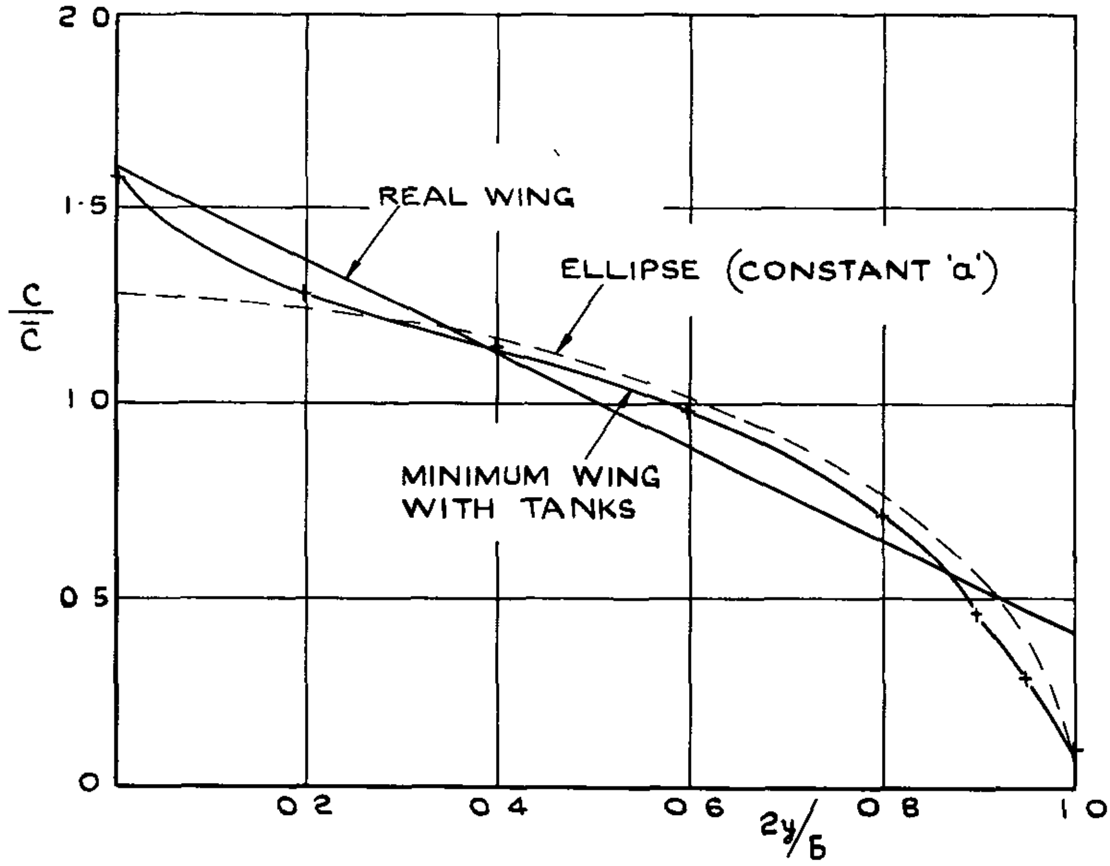

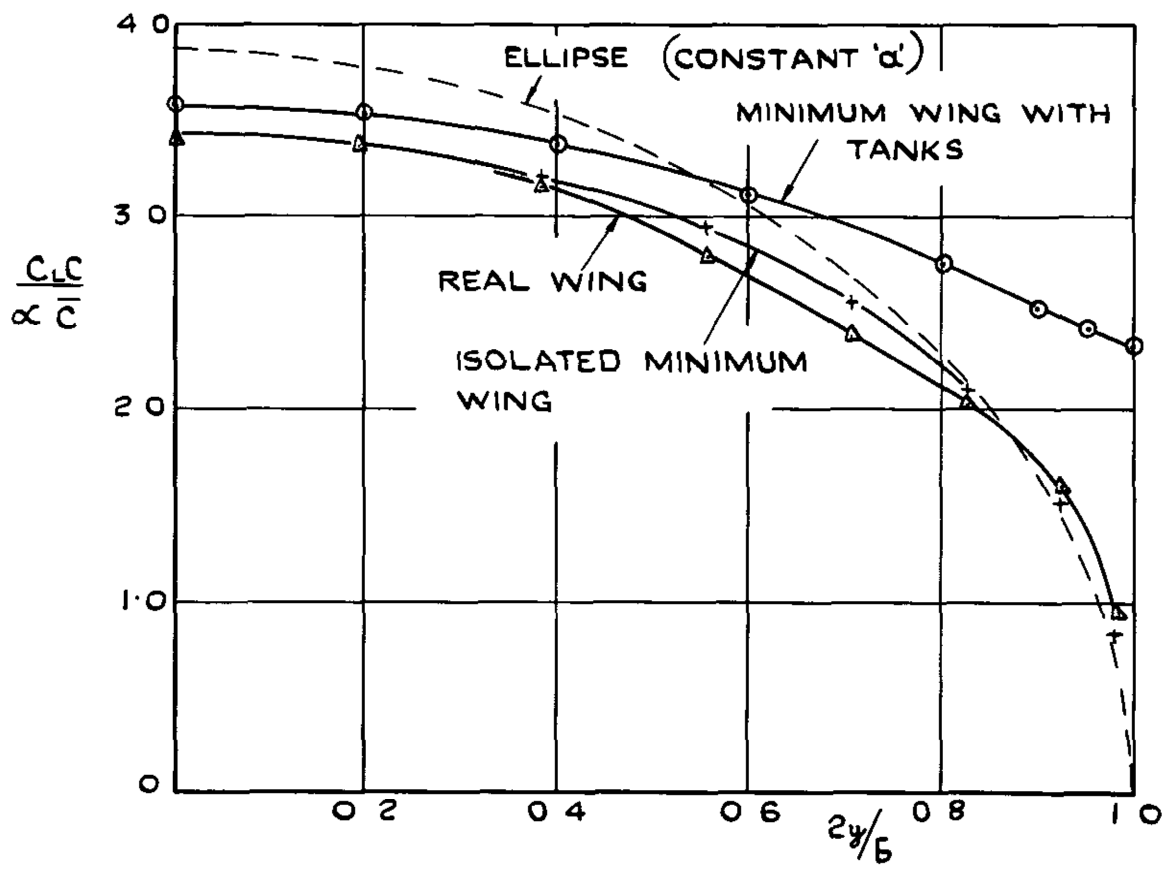

FIG. 21. PLANFORMS AND WING LOADINGS FOR A 59° SWEPT WING, A = 3·61, WITH TANKS $2D/b = 0{\cdot}15$, BY A MORE PRECISE CALCULATION UTILISING VALUES OF THE SECTION LIFT-CURVE SLOPE, 'a', APPROPRIATE TO THE REAL WING (STRAIGHT TAPER; $\frac{\text{TIP CHORD}}{\text{℄ CHORD}} = 0{\cdot}25$)

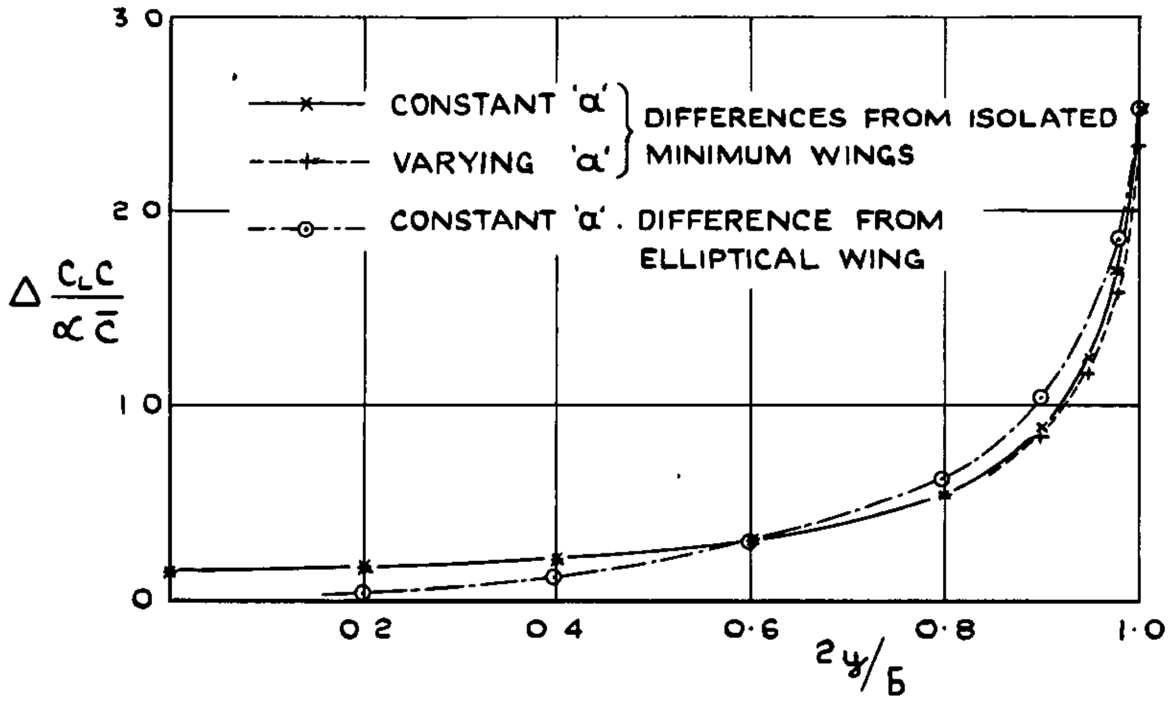

FIG. 22. INCREMENTS IN WING LOAD DUE TO TANKS $2D/b = 0 \cdot 15$ ON A 59° SWEPT WING, $A = 3 \cdot 61$, BY THE APPROXIMATE AND MORE PRECISE CALCULATIONS.

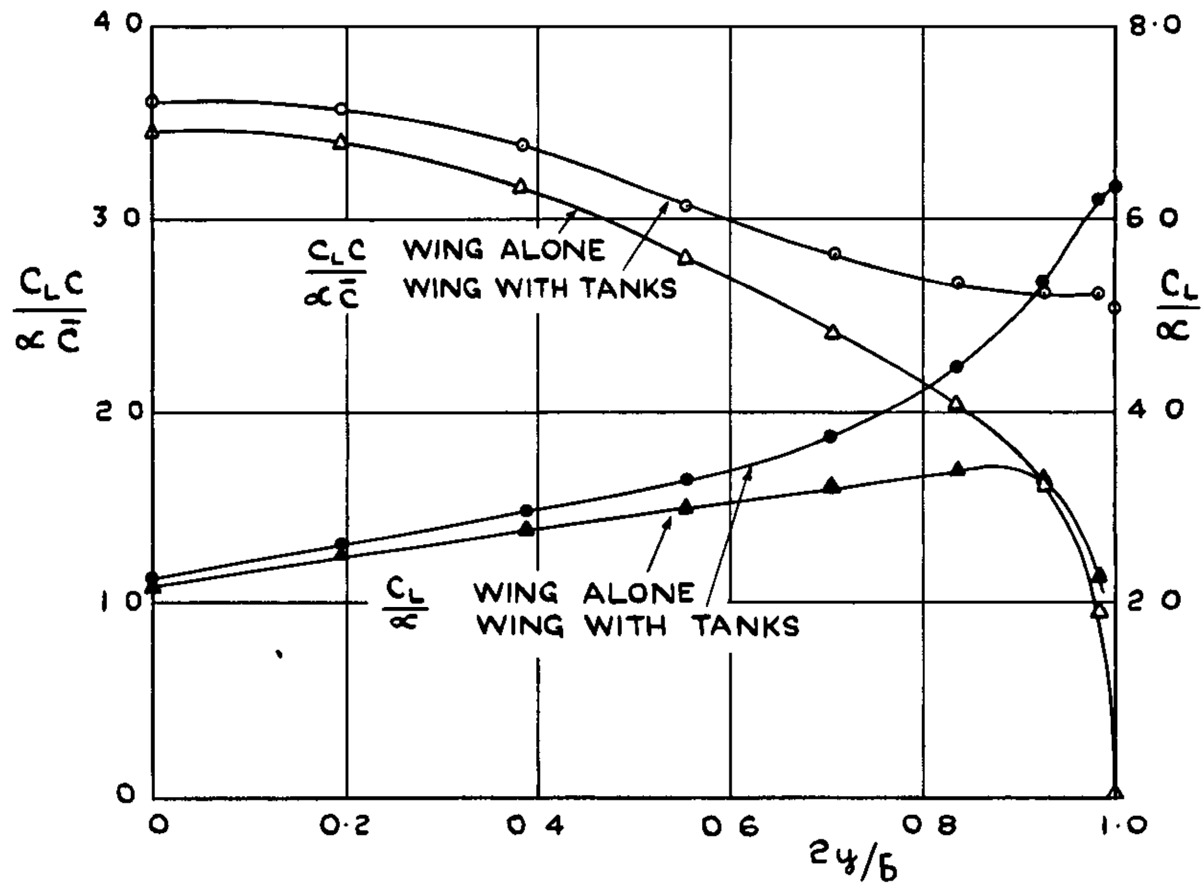

FIG. 23. DISTRIBUTIONS OF WING LOAD AND LIFT-COEFFICIENTS ON A STRAIGHT-TAPERED 59° SWEPT WING, $A = 3 \cdot 61$, WITH AND WITHOUT TIP-TANKS, $2D/b = 0 \cdot 15$.

C.P. No. 147
(15,429)
A.R.C. Technical Report

PUBLISHED BY HER MAJESTY'S STATIONERY OFFICE

To be purchased from

York House, Kingsway, LONDON, W.C 2. 423 Oxford Street, LONDON, W 1
P.O Box 569, LONDON, S.E 1

13a Castle Street, EDINBURGH, 2 | 1 St. Andrew's Crescent, CARDIFF
39 King Street, MANCHESTER, 2 | Tower Lane, BRISTOL, 1
2 Edmund Street, BIRMINGHAM, 3 | 80 Chichester Street, BELFAST

or from any Bookseller

1954

Price 3s. 6d. net

PRINTED IN GREAT BRITAIN

S.O. Code No. 23-9007-47